TRIBHUVAN UNIVERSITY
INSTITUTE OF ENGINEERING
PULCHOWK CAMPUS

THESIS NO: 079/MSPSE/001

Experimental Investigation of the Surface Dielectric Strength of Insulating Tubes Supporting Air Terminals of Electrically Insulated Lightning Protection Systems under Standard Lightning Impulse Voltages

by

Akrit Acharya

A THESIS
SUBMITTED TO THE DEPARTMENT OF ELECTRICAL ENGINEERING IN PARTIAL FULFILLMENT OF THE REQUIREMENTS FOR THE DEGREE OF MASTER OF SCIENCE IN POWER SYSTEM ENGINEERING

DEPARTMENT OF ELECTRICAL ENGINEERING
LALITPUR, NEPAL

APRIL 2025

Experimental Investigation of the Surface Dielectric Strength of Insulating Tubes Supporting Air Terminals of Electrically Insulated Lightning Protection Systems under Standard Lightning Impulse Voltages

By
Akrit Acharya
Roll No: PUL079MSPSE001

Thesis Supervisor:
Associate Professor Dr Basanta Kumar Gautam
Department of Electrical Engineering
Pulchowk, Nepal

A Thesis
Submitted to the Department of Electrical Engineering in partial fulfillment of the requirements for the Degree of
Master of Science in Electrical Engineering in Power System Engineering

Department of Electrical Engineering
Institute of Engineering, Pulchowk Campus
Tribhuvan University
Lalitpur, Nepal
April 2025

DECLARATION AND AUTHORIZATION

This statement formally certifies that the enclosed thesis represents the candidate's authentic and independent research, undertaken solely by them and not previously presented for any other academic qualification or used to obtain a prior degree. It further grants the Institute of Engineering, Pulchowk Campus, explicit permission to disseminate this work for scholarly purposes, including lending copies to other institutions or individuals, and reproducing it through photocopying or other means, in its entirety or in part, ensuring its availability for academic research.

.....

Candidate
Akrit Acharya
PUL079MSPSE001
Department of Electrical Engineering
Pulchowk Campus

.....

Supervisor
Assoc. Prof. Dr. Basanta Kumar Gautam
Head of Department
Department of Electrical Engineering
Pulchowk Campus

COPYRIGHT©

त्रिभुवन विश्वविद्यालय
TRIBHUVAN UNIVERSITY
इन्जिनियरिङ्ग अध्ययन संस्थान
INSTITUTE OF ENGINEERING
पुल्चोक क्याम्पस
PULCHOWK CAMPUS
DEPARTMENT OF ELECTRICAL ENGINEERING
Pulchowk, Lalitpur

Accredited by University Grants Commission (UGC) Nepal 2020

CERTIFICATE OF APPROVAL

The undersigned certify that they have read and recommended to the Institute of Engineering for acceptance, a dissertation entitled **"Experimental Investigation of the Surface Dielectric Strength of Insulating Tubes Supporting Air Terminals of Electrically Insulated Lightning Protection Systems under Standard Lightning Impulse Voltages"**, submitted by **Akrit Acharya** in partial fulfillment of the requirement for the award of the degree of **Master of Science in Power System Engineering**.

Bodh Nath Neupane
Assistant Manager
Nepal Electricity Authority
(External Examiner)

Asst. Prof. Dr. Bishal Silwal
Program Coordinator
M.Sc. in Power System Engineering
Department of Electrical Engineering
Pulchowk Campus, Lalitpur

Assoc. Prof. Dr. Basanta K. Gautam
Head of Department
Department of Electrical Engineering
Pulchowk Campus, Lalitpur
(Supervisor)

April 2025

Tel: +977-1-5443081, Email: doee@pcampus.edu.np, Website: www.doee.pcampus.edu.np

ACKNOWLEDGEMENT

I would like to express my deepest gratitude to my supervisor Associate Prof. Dr. Basanta Kumar Gautam, for his invaluable guidance, insightful comments, and continuous support and encouragement throughout the progress of this research work. Furthermore, I am immensely thankful to Prof. Dr. Nava Raj Karki, Asst. Prof. Yuba Raj Adhikari, Asst. Prof. Anil Panjiyar, Asst. Prof. Dr. Bishal Silwal and the whole team of Department of Electrical Engineering, IOE, Pulchowk Campus for providing the necessary resources and environment conducive to academic growth and learning.

I am also grateful for the opportunity to participate in student mobility funded by Erasmus International Student Program of the European Union. This experience not only enriched my academic journey but also broadened my perspectives, allowing me to engage with diverse cultures and academic traditions. The financial support provided under this project made it possible for me to pursue this invaluable learning experience abroad.

I express my sincere thanks go to School of Electrical and Computer Engineering, Electrical Sector, High Voltage Laboratory at Aristotle University of Thessaloniki, Greece and to Prof. Pantelis N. Mikropoulos and Petros P. Tsouris for their precious suggestion and kind support throughout this research work.

Lastly, I would like to extend my appreciation to my friends and family for their unwavering encouragement and understanding during this challenging yet rewarding endeavor. Their moral support has been a constant source of strength throughout my academic pursuits.

This thesis would not have been possible without the contributions and support of all those mentioned above. Thank you all for believing in me and for being part of this journey.

ABSTRACT

Lightning Protection Systems (LPS) are engineered to protect physical structures, electrical systems, and personnel from the deleterious consequences of lightning strikes. Insulating tubes that support the air termination represent an essential component as they provide electrical isolation for the structure and ensure that current is directed in the desired manner. These insulating tubes must endure significant shock levels during lightning strikes, which can reach hundreds of kilovolts. To verify that they retain their insulating properties, it is imperative to examine the performance of these tubes under standardized lightning impulse voltage conditions. The performance characteristics of these tubes are affected by a multitude of factors, including the polarity of the applied voltage, the composition of the material, the geometry of the tube, and environmental conditions, all of which should be judiciously considered when selecting tubes for practical applications. Standard lightning impulse voltages are distinguished by their extremely short duration and elevated peak voltages, typically characterized as 1.2/50 μs. The response of the tube under such conditions must be integrated into the assessment since the behavior under steadily increasing voltage differs markedly from that under rapidly applied voltage. Consequently, testing in accordance with lightning impulse conditions is essential to ascertain that the materials can withstand the swift voltage escalation and the transient nature of the lightning strike. The failure of insulating stand-offs under lightning impulse voltages can precipitate the failure of the entire lightning protection system. This paper encompasses laboratory investigations aimed at evaluating the dielectric properties of insulating tubes subjected to lightning strikes (both positive and negative) and elucidating their behaviors. The assessment of the surface dielectric strength of electrically insulating tubes is pivotal for enhancing the understanding of the systems reliability, especially in the context of lightning strike scenarios.

Keywords: Lightning Protection System, Insulating Tubes, Air Termination, Marx Generator, Dielectric Strength

TABLE OF CONTENTS

LIST OF FIGURES

LIST OF TABLES

LIST OF ABBREVIATIONS

EILP Electrically Insulated Lightning Protection systems

HV High Voltage

IT Insulating Tube

LI Lightning Impulse

LPS Lightning Protection System

OV Over Voltage

SI Switching Impulse

CHAPTER ONE: INTRODUCTION

Research dealing with surge protection in high voltage equipment reveals the need for further investigation of air gap breakdown characteristics. Although air gaps have been known and studied for decades, continued research shows their importance in the design of new insulating devices. The combination of the simplicity that characterizes air-gap arrangements and the existing knowledge of their properties makes them a basis for the study of more complex arrangements. More generally, the equipment components that make up electricity generation or transmission system must withstand, in addition to the continuous stress from the operating voltage, the stress from the various overvoltage that appear in the system. In order for the high-voltage equipment components to be tested before their use in the laboratory, to ensure their withstand to the various overvoltage that may be observed, prospective surge overvoltage are simulated in the laboratory through impulse high voltages [1].

According to IEC 60060-1:2010 [2], an impulse is any deliberately imposed aperiodic voltage or current pulse, which usually increases quickly to a peak and then gradually declines to zero. Impulse high voltages, depending on the time duration of their front, are categorized into lightning (LI) and switching (SI). Lightning impulse high voltages are those in which the front duration is less than 20μs, while on the contrary the front duration of switching impulse high voltages is longer than 20μs.

In electrical engineering, overvoltage is the state in which the voltage in an electrical system is higher than the rated or typical operating voltage. This may be caused either by external overvoltage or internal overvoltage which may result in system instability, insulation failure or equipment damage.

1.1 Theoretical Background

1.1.1 External Overvoltage

It is caused by external sources, mostly natural events like lightning strikes, which produce brief, high-energy voltage spikes. Switching operations on large-scale transmission lines or electromagnetic interference can also cause this overvoltage. Some of the causes for external overvoltage are direct lightning strokes, electromagnetically induced over voltages

due to lightning discharge taking place near the line, called 'side stroke', voltages induced due to atmospheric changes along the length of the line and electrostatically induced voltages due to presence of charged clouds nearby.

Although external overvoltage usually only last a few milliseconds to microseconds, they can reach very high magnitudes and pose serious dangers to insulation and equipment. Surge arresters, shielding, and efficient grounding are methods of mitigating external overvoltage to safely levels. This type of overvoltage originates from atmospheric disturbances, mainly due to lightning. This takes the form of a surge and has no direct relationship with the operating voltage of the line. Lightning impulse high voltages are defined as having a front duration of less than 20 s and simulate external surge overvoltage in the laboratory. Lightning impulse high voltages are characterized by the amplitude or peak voltage Up, the front duration T1 and the half-width duration T2. Because of stray inductances and capacitances on the components of the generating and measuring devices of the system, the exact determination of the peak voltage as well as the duration of the front of a generated external high voltage becomes difficult. According to Mikropoulos in [1], the front duration can be calculated as:

$$T_1 = 1.67 \times T \tag{1.1}$$

where T, the interval between the time instants corresponds to 30% and 90% of the peak voltage value. For the same reasons, the half-width duration of a high-voltage impulse is in turn a conventional parameter defined as the time interval from the conventional beginning of times to the time when the voltage decreases to 50% of the peak voltage value.

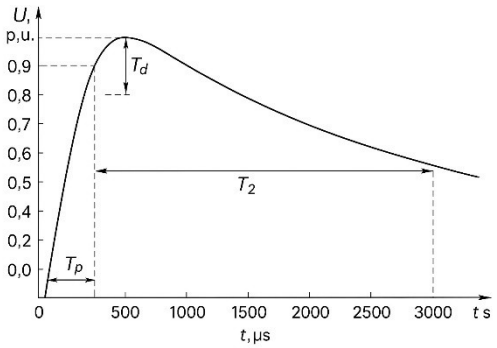

Figure 1. 1 Sample Switching Impulse

Lightning Phenomenon

Lightning is a natural phenomenon which occurs stepping electric charge between the clouds with the earth. If the charge in the cloud grows, the greater the induced charge so that the potential difference between the clouds with the earth becomes even greater. The incident was followed by the release of the electron charge in the form of tongues of lightning that came down from the clouds and up from the earth [4,5]. This can produce electromagnetic radiation, including heat and visible light flashes. Thunderstorms occur when warm air masses with moisture are transported to high altitudes. This can occur through heat thunderstorms, frontal thunderstorms, orographic thunderstorms. Heat thunderstorms involve intense insolation, while frontal thunderstorms involve cold air front invasion, pushing cooler air below warm air. Orographic thunderstorms occur when warm air near the ground is lifted. Electrostatic charge separation processes charging water droplets and ice particles, with positive and negative charges. Thunderstorms generate corona discharge from ground objects, transported by wind. If space charge densities in a thundercloud produce strong local field, leader discharges initiate lightning discharges. Cloud-to-cloud flashes neutralize charge between cloud and ground centers, but their electromagnetic impulses pose a threat to electrical and electronic systems. Flashes to earth neutralize charge between cloud and ground charges, with two types distinguishable.

Downward flashes (cloud to earth flash) involve lightning discharges from the cloud to the ground, typically occurring in flat terrain and near low buildings. Cloud-to-earth flashes can be identified by the branching directed to earth. The most common type is a negative downward flash, where a leader filled with negative cloud charge pushes its way from the thunder cloud to earth. Upward flashes (earth to cloud flash) occur on high, exposed objects or mountain tops, triggering a leader by the distortion of the electric field on the exposed object. Upward flashes occur with both negative and positive polarity. Since, with upward flashes, the leaders propagate from the exposed object on the surface of the earth to the cloud, high objects can be struck several times by one lightning discharge during a thunderstorm. Figure 1.2 shows the standard lightning impulse waveform.

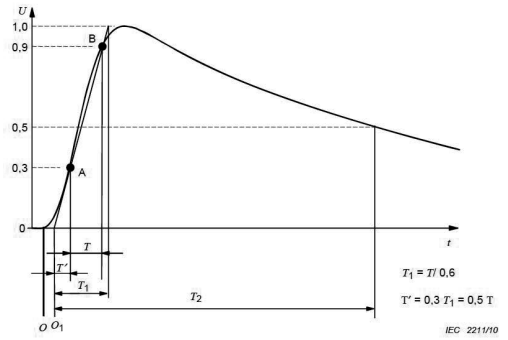

Figure 1. 2: Sample Lightning Signal

Lightning Surges

A lightning surge is the sharp, transient electrical pulse generated during a lightning strike, characterized by high voltage and current. This impulse can cause electrical surges, damage to infrastructure, and interference with electronics. In the lab, impulse high voltages replicate surges that might happen in an electrical power supply because of lightning strikes. IEC 60060-1:2010 [2] defines an impulse as any purposefully induced aperiodic pulse of voltage or current that typically increases quickly to its maximum and then gradually decays to zero. Impulse high voltages are classified as internal (SI) or external (LI) based on the duration of time their front lasts. External high voltages have a front duration of less than 20 μs, whereas internal high voltages have a front duration of more than 20 μs.

1.1.2 Internal Overvoltage

Internal overvoltage in electrical engineering refers to an increase in voltage within an electrical system, caused by events or conditions originating inside the system. Unlike external overvoltage, which are typically caused by external factors like lightning, internal overvoltage result from system operations, faults, or equipment interactions.

1.1.3 Lightning Protection System

A Lightning Protection System (LPS) is designed to safeguard structures, electrical systems, and personnel from the damaging effects of lightning strikes. It works by intercepting lightning and safely channeling the high-energy current to the ground, minimizing the risk of structural damage, electrical surges, and fire. When lightning strikes,

the system intercepts the lightning through air terminals. The current is conducted through the down-conductors to the grounding system, which dissipates the energy safely into the earth. Surge protection devices protect the internal electrical systems from overvoltage caused by lightning. Among the various components that comprise LPS, electrically insulated lightning protection systems (EILPS) stand out as essential features, particularly for ensuring the safe passage of lightning energy through the system while preventing damage to the structure and its electrical systems.

A Lightning Protection System (LPS) is vital in electrical engineering to protect infrastructure, equipment, and lives from lightning strikes. It prevents structural damage, fires, and voltage surges by safely diverting lightning currents to the ground. LPS also safeguards sensitive electrical systems, ensures human safety, reduces downtime, and ensures compliance with safety standards, making it critical for reliable and uninterrupted operations, especially in critical facilities like hospitals and power plants.

An isolated lightning protection system is designed to separate the current lightning path from the protected structure, ensuring no interaction occurs between the lightning and the building. This is achieved by using free-standing air terminals or masts placed at a safe distance from the structure, with the lightning current directed to the ground through external conductors. Isolated systems are ideal for high-risk facilities like oil storage tanks or chemical plants, where preventing side-flashing is critical.

An electrically insulated lightning protection system uses conductors covered with high-voltage-resistant insulating materials or maintains a safe distance between the lightning path and the structure. This system is particularly suited for buildings with rooftop equipment, such as solar panels or HVAC units, as it prevents arcing and electromagnetic interference. Both systems aim to protect the structure and its components while minimizing the risks associated with lightning strikes, with the choice depending on the facility's specific needs and risks.

1.1.4 Components of Lightning Protection System (LPS)

The list of components of lightning protection systems are [16]:

Air Termination

One essential part of a lightning protection system (LPS) is an air termination system. Its purpose is to securely transfer high-voltage electrical energy to the ground via a specified path after intercepting lightning strikes. This reduces the possibility that the building and its people may sustain harm. They are installed on a free-standing poles or masts located at a safe distance from the protected structure. They are mainly made from highly conductive materials such as copper or aluminum to ensure effective lightning capture. The height and place of the air terminals are calculated based on the area of protection and the height of the structure (standards like IEC 62305) [3].

The air termination system comprises of air-termination rods (lightning rods), meshed conductors or cables, air termination mesh and natural components. Air termination rods are tall, pointed conductors typically installed on the highest parts of a building or structure. They are made of conductive materials like copper or aluminum. The main motive for this is to act as the first point of contact for lightning strikes. The meshed conductor can be taken as a network of conductors installed across the structured roof. It should ensure comprehensive coverage to capture lightning regardless of where it strikes. Air termination mesh is a gridlike structure of conductors that are spread over the roof to intercept lightning. They are used for larger or more complex roofs. The natural components are metallic structures on the building such as HVAC units, antennas, or metallic roofs can also act as a part of the air termination system, provided they are suitably interconnected.

Down-conductors

The down-conductors are a critical component of a lightning protection system (LPS). They provide a low-resistance path for the lightning current to travel safely from the air termination system to the grounding system. This helps to minimize the risk of side-flashing, structural damage, and fire hazards caused by lightning strikes. Similarly, multiple conductors ensure lightning current division and that if one path is damaged or overloaded, the current is still safely directed to the ground. Down-conductors are installed externally away from the structure to maintain isolation. They are made from copper or aluminum with high conductivity and corrosion resistance. They are routed vertically and in a direct path to the ground to minimize inductance and potential arcing.

The components of down conductors are clamps and fasteners, bonding elements, inspection points as well as spark gaps and surge arresters as an optional component. Clamps and fasteners ensure the secure connections of the conductors to the building and prevent damage due to movement. Bonding elements ensure a safe connection between the down conductors and other metallic parts of the structure. Inspection points are the accessible locations for periodic maintenance and testing. Spark gaps and surge arresters protect sensitive electrical systems by safely diverting excessive voltage.

Grounding System (Earth Termination System)

The grounding system, also known as the earth termination system, is a crucial component of a lightning protection system (LPS). It serves to safely dissipate the enormous electrical charge from a lightning strike on the earth, preventing damage to structures, equipment, and human beings. It comprises earth electrode, conductors, connection to earth and bonding. Earth electrodes are metallic rods, plates, or conductors placed in the ground to provide a low-resistance path for lightning currents to flow safely into the earth. It may be ground rods which are vertical conductive rods driver into the earth usually made of copper or copper bonded steel, ground plates or mesh which are horizontal components used in areas where deep grounding is not possible or ring grounding system which encircles the structure for better dissipation and to equalize potential around the structure. The down conductors (usually copper or aluminum) run from the lightning protection system's air terminals (lightning rods) to the earth electrodes. These conductors carry the lightning current from the structure to the grounding system. The earth electrodes are typically installed in areas with low resistivity, such as moist soil, to ensure a good electrical connection to the ground. The goal is to reduce the resistance of the earth connection to the lowest possible value to allow the lightning current to flow without creating dangerous potential differences. Proper bonding ensures that all metal parts of the structure (e.g., water pipes, HVAC systems, and steel beams) are electrically connected to the grounding system. This prevents dangerous step voltages from occurring, which could harm people or damage equipment.

An insulating component in a lightning protection system (LPS) is used to prevent or minimize the risk of sparking or dangerous electrical currents between the lightning

protection conductors and nearby conductive structures or installations. These components are essential for ensuring safety, particularly in areas where the LPS is installed near sensitive or hazardous materials or in systems with high electrical potential differences. They are made of high voltage resistant materials such as fiberglass, ceramics, or composite polymers.

Support structures

A support structure in a lightning protection system (LPS) is designed to securely hold and guide the components of the system, such as air terminals, conductors, and down-conductors, in place while ensuring optimal functionality and safety. It provides the necessary mechanical stability to withstand environmental stress like wind, precipitation, or thermal expansion. Mounting bases and holders, conductor supports, masts and poles, clamps and fasteners and insulated standoff brackets are the components of support structures. The mounting bases and holders are used to attach air terminals, conductors, or rod to buildings surfaces like roofs or walls. They are usually made of stainless steel, aluminum, or weather-resistant plastics. The conductor supports ensure conductors are firmly positioned along walls, roofs, or other surfaces. They provide insulation where necessary to avoid contact with conductive building parts. Mast and poles elevate air terminals to ensure coverage of the protected zone. They are made of non-corrosive and durable materials such as galvanized steel, fiberglass, or aluminum. The clamps and fasteners secure the connection of various components to the support structure and maintain electrical continuity while providing mechanical rigidity. The insulated standoff brackets provide separation between conductive components and nearby structures to prevent arcing. They are commonly used in areas with high potential differences.

1.2 Problem Statement

The problem statement can be listed as:

i. The surface dielectric strength of electrically insulating tubes supporting air terminal in lightning protection systems under simulated lightning impulse conditions is insufficiently studied.
ii. Lack of comprehensive studies on flashover characteristics may lead to inadequate lightning protection and system failures.

iii. Uncertainty in material performance under lightning impulse conditions necessitates testing their surface dielectric strength.
iv. Understanding surface dielectric strength is crucial for designing effective lightning protection systems.
v. Poorly selected or inadequate insulating stand-offs can compromise the protection of structures and systems.

1.3 Objectives

1.3.1 Primary Objective

The primary objective of this study is to experimentally investigate the surface dielectric strength of electrically insulating tubes used to support air terminals in electrically insulated lightning protection systems (EILPS) when subjected to standard lightning impulse voltages

1.3.2 Secondary Objective

i. To evaluate the surface dielectric strength of various insulating materials used in lightning protection systems when subjected to lightning impulse voltages.
ii. To simulate insulating tube model on COMSOL and evaluate the internal and external electric field.
iii. To find the effect of permittivity on the internal and external electric field.

1.4 Scope

- Material focus

The study focused on commonly used electrically insulating tubes supporting air terminals in EILPS, including polymers and composite materials. I evaluated the surface dielectric strength characteristics of materials under controlled laboratory conditions

- Experimental Setup

Utilized standardized lightning impulse voltage waveforms (1.2/50 μs) of both positive and negative polarities produced by Marx Generator. Conduct tests on insulating tubes with varying dimensions and configurations were performed.

- Parameters Evaluated
    i. Surface dielectric Strength
    ii. Flashover Voltage
    iii. Peak flashover Current
    iv. Time to flashover
    v. Flashover probability distributions
    vi. Flashover voltage-time characteristics

1.5 Limitation

i. Controlled Conditions: Tests conducted were under controlled laboratory conditions, which may not fully replicate real-world environmental factors.

ii. Material Selection: The study mainly focused on a limited range of insulating materials and did not cover all materials used in industry.

iii. Impulse Waveform: Only standard lightning impulse voltages (1.2/50 μs) were tested, excluding non-standard waveforms.

iv. Long Term Effects: The investigation did not include long-term aging effects or degradation mechanisms of the insulating tubes over time.

1.6 Thesis Organization

The structure of the thesis is the following:

i. In the first chapter, the introduction of the dissertation, some necessary theoretical data are mentioned regarding high impulse voltages, electrically insulated lightning protection systems and the insulating tubes supporting their air terminals. A brief description of the physical interpretation of the phenomenon of electrical breakdown is also attempted, accompanied by a brief literature review on the effect of the affecting factors on the breakdown mechanism.

ii. In the second chapter, the High Voltage Laboratory of Aristotle University of

Thessaloniki, where the experiments were conducted, is presented, together with a detailed description of the experimental equipment and arrangement.

iii. In the third chapter, the simulation investigation of electric field was evaluated using COMSOL.

iv. In the fourth chapter, the experimentally obtained flashover characteristics are defined, and the experimental procedure is detailed described.

v. The fifth chapter deals with the presentation and commentary of the experimental results. The experimental data on flashover characteristics are evaluated as affected by the amplitude and polarity of the applied voltage as well as by the material and the geometrical configuration of the insulating tubes under test.

vi. In the sixth chapter, the conclusions of the thesis are presented.

vii. The seventh and final chapter consists of suggestions for future research.

1.2 Literature Review

Electrically insulated lightning protection systems, LPS, are used when the flow of lightning current may cause damage to the structure under protection or its contents, as well as dangerous sparking to its internal conductive parts [6]. In protecting buildings from lightning, we must bear in mind that it does not follow the law of electric currents such as we are familiar with or those we read about as being employed for long distance power transmission. Lightning shows a great tendency to distribute itself over such conductors as may be present on a building, and in doing so pays little heed to ohmic resistance. It finds no great difficulty in making its way, often for a considerable distance, through the air or any other medium of rather better conductivity. It prefers as much as possible to move in a straight line, and that therefore sharp turns, bends, or spiral windings in conductors readily lead to lateral discharges [7].

IEC 62561 currently exists of 7 parts covering such components as clamps and conductors, conductors, air termination rods, earth electrodes, conductor fasteners, isolating spark gaps, and soil improvement compounds. Additional work is under consideration on a standard on components for isolated protection systems [8]. The research and analysis for the lightning stroke is important for these components. They are mainly used for protection of

buildings and other components for lightning. If any component failure during the lightning stroke, the stroke cannot go to the earth safely and may go through the unintended part causing the issue. An air terminal with an insulating tube typically consists of a conductive metal (like copper or aluminum) rod or terminal that is surrounded by a non-conductive insulating tube. The tube is usually made of materials such as polymer composites, ceramics, or insulating rubber.

This insulating layer serves multiple purposes. It isolates the air terminal from the structure, preventing any unwanted electrical transmission along the terminal to other parts of the building. The insulating tube provides an additional protective layer, reducing the exposure of the terminal to corrosive elements in the environment. Insulating materials protect the metal from direct contact with the external environment, reducing the likelihood of damage due to environmental factors like moisture, chemicals, or salt. The insulating tube can help in reducing the possibility of side flashover, where lightning energy may arc from the air terminal to the structure.

Air terminals with insulating tubes showed higher durability in coastal areas with high humidity and salt exposure. Electrical isolation reduced the potential for side flashovers, providing enhanced protection for nearby electrical systems [9]. The insulating tube significantly reduces the possibility of lightning-induced surges entering the electrical system, which could otherwise lead to costly damage or fire hazards. Insulating tubes enhance the efficiency of the lightning protection system by ensuring that lightning energy follows the designed pathway (normally an insulating down-conductor) to the ground. The introduction of insulating tubes made air terminals significantly safer by providing electrical isolation, especially in environments with sensitive electrical systems like telecommunications towers and data centers [10].

Traditional air terminals are prone to side flashing and stray current issues, which can damage nearby equipment or pose risks to personnel. By incorporating insulating tubes, the risk of unintended current flow is minimized, ensuring that the lightning current follows a controlled path to the ground through an insulating down-conductor. The study presents experimental tests and simulations under varying conditions to compare the performance of insulated air terminals against conventional designs. Mainly the paper focuses on

methods for determining protected volumes and configuring air-termination systems using mathematical calculations and graphical simulations, primarily involving lightning rods [11].

The breakdown characteristics of the high voltage test are mainly performed with multi-level test. The multiple-level method (MLM) means the application of constant voltage tests at several voltage levels. For each level the test delivers an estimation of the breakdown probability including its confidence limits [12]. According to Kuffel in [13], basic procedure of the multi-level test is

1. choose several test voltage levels
2. apply a pre-specified number of shots at each level (n),
3. count the number (x) of breakdowns at each voltage level
4. plot p(V) (x_j/n) against V (kV),
5. draw a line of best fit on a probability scale,
6. from the line determine V_{50} at z=0 or P(V)=50 per cent,
7. and σ at z=1or $\sigma=V_{50\%} - V_{16\%}$

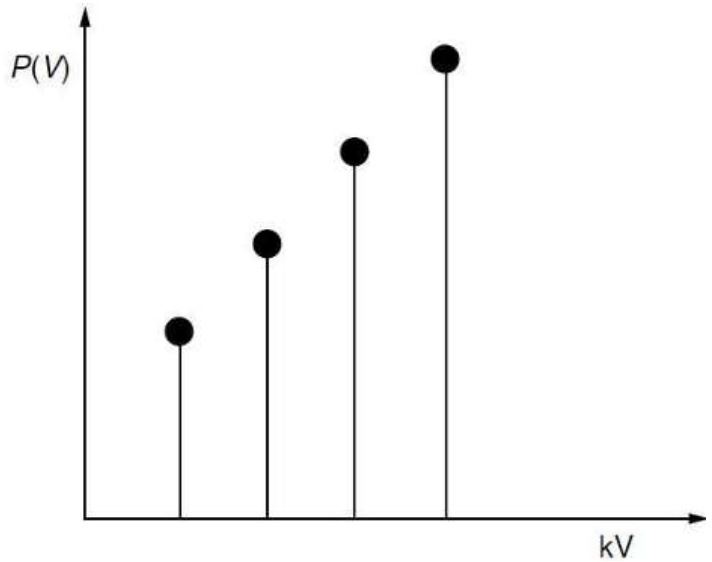

Figure 1. 3 Probability of breakdown distribution using the multi-level method

The recorded probability of breakdown, x_j/n, is the number which resulted in breakdown from the application of n shots at voltage Vj. when xj/n is plotted against Vj on a linear

probability paper a straight line is obtained as shown in figure 1.3. The advantage of this method is that it does not assume normality of distribution. The disadvantage is that it is time-consuming, i.e. many shots are required [13].

The 50% lightning impulse breakdown voltage is significant in lightning protection as it determines the voltage level at which insulation systems can fail, ensuring that protective measures are designed to withstand these conditions, thereby enhancing safety and reliability [14].

So as insulating tubes enhance the overall performance and safety of air termination systems by isolating the lightning strike path, reducing side flashing, and preventing interference with sensitive equipment. These advantages make them crucial in designing lightning protection systems for sensitive and high-risk environments, it is important to find the flashover characteristics of the insulating tubes used in the air termination system. The surface dielectric strength of electrically insulating tubes supporting air terminal in lightning protection systems under simulated lightning impulse conditions is insufficiently studied. There is lack of studies on the flashover characteristics of the insulating tubes used in the air termination and that may lead to inadequate lightning protection and system failures Similarly, the dimensions and the material used as the insulating tubes has an crucial role in the protection. Proper research and analysis have not been done on those parameters.

Air terminals prevent direct lightning strikes to structures, significantly reducing the risk of ignition in sensitive areas, such as cold vent stacks in the oil and gas industry [15]. This research mainly demonstrates the flashover characteristics of the insulating tubes supporting the air terminals. 3 different types of insulating tubes with different characteristics (dimensions and materials) are under test and analysis of each insulating tube is carried out. Finally, the comparison between those insulating tubes and their characteristics are to be made for the safety of the system under protection. The flashover probability distribution is performed using the multi-level test method.

CHAPTER TWO: EXPERIMENTAL SETUP AND EQUIPMENT

2.1 High voltage laboratory area

The experimental measurements during this thesis were carried out in the High Voltage laboratory of the Aristotle University of Thessaloniki, specifically in the main High Voltage testing area of the laboratory. The laboratory was founded in 1984 and serves educational and research needs in the subject of High Voltages. The laboratory includes two High Voltage test areas as well as corresponding control and measurement areas. It also has an auxiliary laboratory, office and warehouse spaces. The main test area is completely enclosed by means of a ground metal mesh in all its dimensions. The metal cage is 6.5 m high, 12 m long and 7 m wide. A lab's ability to produce high voltages is limited by the dimensions of the lab itself. The experimental measurements were carried out in the main testing area of the laboratory, which is completely enclosed in a grounded metal mesh in all dimensions (Faraday cage), to avoid the inadvertent entry of personnel and to reduce the electromagnetic noise in the quantities under measurement.

The height of the metal cage, which is also the minimum of the dimensions of the main testing area, is what determines the limits to the laboratory's ability to produce high voltages. The minimum safety distance of 3.25 m limits the possibility of producing high voltages at values depending on the type of voltage. For high voltage alternating current (HVAC) the maximum value is 650 kV (rms), for high direct current (HVDC) 900 kV, for switching impulse high voltages (SI) 1 MV and for lightning impulse high voltages (LI) 1.4 MV.

The main area of the laboratory provides the necessary security for both its staff and its visitors. The doors leading to the high voltage laboratory have a hazard warning sign and indicator lights that indicate whether the high voltage equipment is electrified (red indicator) or not (green indicator). They are equipped with a safety door switch whose contacts close when the door is closed. The door switches are connected in series with the safety interlock system which automatically cuts off the voltage supply in case any laboratory door is opened and does not allow the voltage supply when any of the entrance doors to the test area are open. Entry to the test area is permitted only when all high voltage equipment components are grounded. Earthing is done by means of an automatic visible contact earther which is activated when the power supply is interrupted. In addition, there

is also a mobile protective earth with a conductive hook, reliably connected to the laboratory earthing installation which is used by the laboratory staff in cases where its use is mandatory.

The floor of the laboratory is covered with metal layer sheets intended to limit the development of potential difference between different points of grounding of equipment or high voltage circuits and especially to limit the development of step voltages. All metal parts of the test area that do not carry high voltage are properly earthed and connected to the laboratory earthing installation through specially designed earthing conductors of suitable cross section. The cables used in the high voltage measurements are coaxial with a reliably grounded shield.

The grounding systems of laboratory include the foundation grounding of the building, the independent protective grounding in the main testing area, which is a grounding rod to which the high-voltage generation and measurement devices are directly connected with a copper grounding tape, as well as other grounding systems such as the automatic earther, the mobile earther and the floor layer sheets mentioned above. The earthing system primarily ensures the safety of staff - visitors and secondarily the safe operation and protection of the equipment.

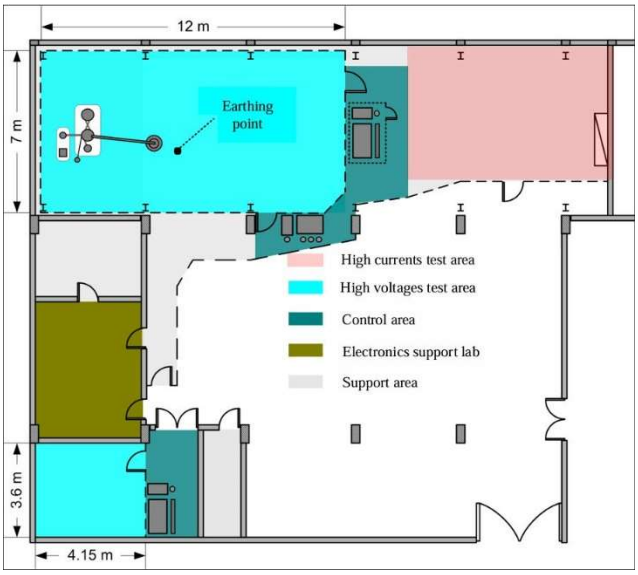

Figure 2. 1: High voltage laboratory area

2.2 Generation and measurement of impulse high voltages

The complete circuit required for high voltage equipment testing consists of:

- The high voltage generation device and the connection to the test
- The essay itself
- The voltage measurement system

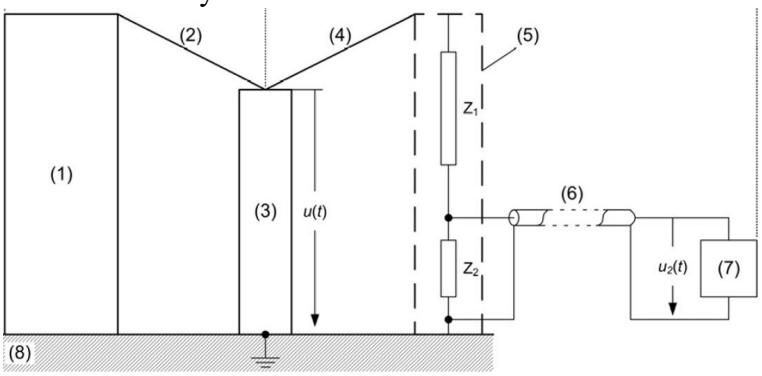

Figure 2. 2: High voltage test circuit

The components of test circuit presented in Fig. 2.2 are listed as follows:

1. High Voltage Generator
2. High voltage generator test connection
3. Test
4. Test-voltage divider connection
5. Voltage Divide
6. Measuring Lead
7. Recorder Voltage
8. Grounded laboratory floor

The high voltage measurement system includes the test connection to the voltage divider, the voltage divider, the measuring cable inserted between the output of the voltage divider and the input of the recording instrument and the recording instrument itself. When testing high voltage surge equipment, the voltage divider is usually a component of the surge generator so as not to load the generator by altering the output waveform.

For the experimental device used in the context of this thesis, the role of the high voltage generator is assumed by the Marx generator (1.2/50 μs). The capacitor of this front performs a double function, i.e. it also serves as a high voltage capacitor of the capacitive

divider. The generated impulse voltage is transferred from the Marx output to the tip of the air termination. The high voltage is applied using the Marx generator and the data such as current and voltage and their waveform is recorded. If there is not any flashover at any voltage level, the next high voltage level is selected. The maximum voltage, time to breakdown, peak current, etc. are measured for the case of breakdown. Figure 2.3 shows the air termination (lightning component under test whereas figure 2.4 shows the lightning impulse from the Marx generator to the air termination. citron and its external resistor AUTH laboratory.

The devices are grounded through a suitable cable that passes through the voltage transformer for current measurement purposes and ends at the ground floor. The output of the current transformer ends up via a suitably shielded cable to the signal attenuator which is connected to the oscilloscope.

Emphasis is placed on recording the waveform of the discharge current, in addition to the waveform of the voltage imposed on the sample. Through recording the current, important conclusions can be drawn about the behavior of the gaps and their breakdown characteristics, as it gives the opportunity to study many factors such as conclusions about the initiation and development of the discharge and generally about the pre-discharge phenomena.

2.2.1 Theoretical elements

The picture below depicts the two fundamental circuits for single-stage high impulse voltage generators. In figure (a), d.c voltage Vo charges the capacitor C_1 till the spark gap 'G' breaks down. Single stage generators can be utilized only for the voltage from some kV to 1 MV. However, the economic charging voltage level Vo is about 200-250 kV. C_1 acts as a smoothing capacitor whereas resistor R_1, R_2 and capacitance C_2 form the wave shaping network. After the spark gap breaks down, R_1 damps the circuit and determines the front time T1 whereas R_2 will discharge the capacitors and control the wave tail. The C_2 represents the full load i.e. the object under study. The inductance is neglected. The output voltage of the generator is the voltage across the capacitor C_2.

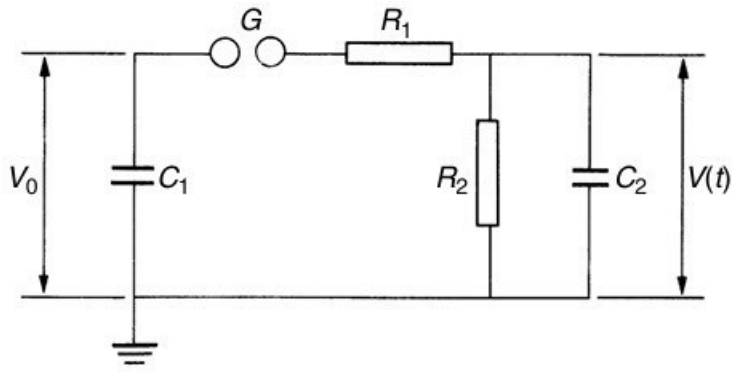

Figure 2. 3: Single stage impulse generator (a)

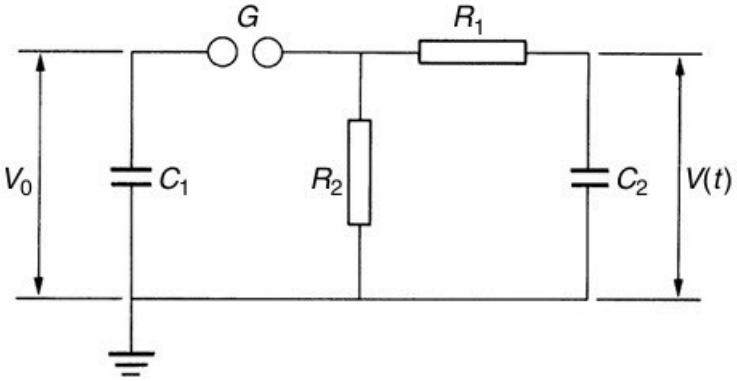

Figure 2. 4:Single stage impulse generator (b)

The generation of impulse voltages requires a rapid increase of the voltage to its maximum value and a slow decrease to its zero value. Circuit-wise this means that the impulse capacitor C_2 needs to be charged quickly, while the parallel combination of C_2 and C_1 needs to be discharged slowly. From Kuffel in [13], these requirements are met as long as

$$R_2 \gg R_1 \; and \; C_1 \gg C_2 \tag{2.1}$$

And the maximum energy stored in a single stage generator is given by:

$$W = \frac{1}{2} C_1 {V_0}^2 \tag{2.2}$$

The Laplace transform is simulated under the boundary condition:

- When $t \leq 0$, C_1 is charged to V_0
- When $t > 0$ this capacitor is directly connected to the wave-shaping network. For the above circuits, the output voltage according to Kuffel in [13] is given by the expression

$$V(s) = \frac{V_0 Z_2}{s(Z_1 + Z_2)} \tag{2.3}$$

where,

$$Z_1 = \frac{1}{C_1 s} + R_1 \tag{2.4}$$

$$Z_2 = \frac{\frac{R_2}{C_2 s}}{R_2 + \frac{1}{C_2 s}} \tag{2.5}$$

then,

$$V(s) = \frac{V_0}{k} \frac{1}{s^2 + as + b} \tag{2.6}$$

where,

$$a = \frac{1}{R_1 C_1} + \frac{1}{R_1 C_2} + \frac{1}{R_2 C_2} \tag{2.7}$$

$$b = \frac{1}{R_1 R_2 C_1 C_2} \tag{2.8}$$

$$k = R_1 C_2 \tag{2.9}$$

For the figure (b), the expression for the output voltage is same however,

$$a = \frac{1}{R_1 C_1} + \frac{1}{R_1 C_2} + \frac{1}{R_2 C_2} \tag{2.10}$$

For both circuits we can obtain the output voltage in time domain as:

$$V(t) = \frac{V_0}{k} \frac{1}{(\alpha_2 - \alpha_1)} [\exp(-\alpha_1 t) - \exp(-\alpha_2 t)] \tag{2.11}$$

where α_1 and α_2 are the roots of the equation $s^2 + as + b = 0$

$$\alpha_1, \alpha_2 = \frac{a}{2} + \sqrt{\left(\frac{a}{2}\right)^2 - b} \tag{2.12}$$

The output voltage V (t) is therefore the superposition of two exponential functions of

different signs. (need to add negative and positive effect)

The figure (a) and (b) defers in terms of the utilization factor (voltage efficiency). Therefore, variations in the values of k=R1 × C2 for both circuits are the only possible cause of the efficiency disparities. The circuit, which always has a better efficiency for a given ratio of C2/C1, can be used to compute this term first because the resistors R1 and R2 do not form a voltage-dividing system during it from Kuffel [13].

For figure (a)

$$\eta = \frac{U_p}{U_0} \leq \frac{R_t}{R_t + R_f} \frac{C_c}{C_c + C_f} \tag{2.13}$$

For figure (b)

$$\eta = \frac{U_p}{U_0} \leq \frac{C_c}{C_c + C_f} \tag{2.14}$$

The generation of the desired impulse voltage waveform is obtained for given values of generator capacitances by using a suitable pair of front and tail resistor values, while the peak value can be varied by controlling the generator charging voltage. If the production of impulse high voltages with a large peak value is desired, then multistage generators or Marx generators are used. The schematic diagram of n-stage Marx generator type b is shown in figure 2.5.

2.2.2 Production of impulse high voltages

2.2.2.1 Marx Generator

Multi-stage generators such as Marx Generators are used to produce large peak value impulse high voltages. The Marx generator is a device proposed by Erwin Otto Marx in 1923. These generators are used to test the strength of electrical equipment such as insulators and transformers at high impulse voltages according to IEC international standards and more generally for simulating lightning strikes and their consequences. As shown in figures, in Marx generators several impulse capacitors, C_c, as many stages of the generator, connected in parallel through load resistors, R_L, are charged to a continuous high voltage and then discharged, through the breakdown of spherical gaps, connected in series on a load capacitor, C_f. In this way the output voltage of the generator is proportional to the number of stages.

Marx generators combine impulse capacitors, front and tail resistors as well as auxiliary spherical gaps in a manner like that of single-stage generators. These elements are usually distributed among the stages of the generator is the same with that of the single-stage generator with equivalent values of elements and charging voltage as shown below: $C_c=C_{cn}/n$, $R_f=n \times Rf_n$, $R_t=n \times Rt_n$, $U_0=n \times U_{0n}$, where the index n denotes the values of the individual elements of the Marx generator. Depending upon the type of circuit, additional front resistance or tail resistance can be added. The ignition of the high voltage impulse generator is done by the breakdown of the auxiliary gap of the first stage which triggers the successive breakdown of the gaps and the remaining stages. The ignition is either automatic or controlled. During its automatic start generator, either a specific value of charging voltage is applied and the distance between the spheres of the auxiliary sphere gap is reduced until breakdown, or the distance between the spheres of the auxiliary sphere gap is set to a specified value and the charging voltage of the generator is increased until the breakdown of the auxiliary gap. Controlled starting of the generator is usually achieved using the Trigatron device, the operation of which is discussed in a later section.

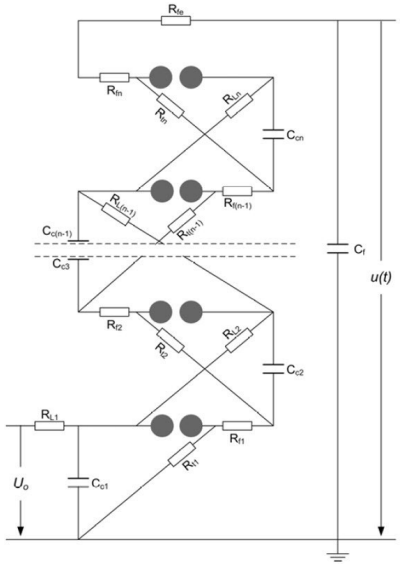

Figure 2. 5: Schematic diagram of n-stage Marx generator type b

The production of the lightning impulse high voltages during the experimental measurements was carried out using the 10-stage Marx generator, manufactured by Ferranti, which is installed in the main testing area of the high voltage laboratory of the AUTH. This generator produces lightning impulse high voltages of waveform 1.2/50s type, which are used to simulate surge overvoltage due to direct lightning strikes. In

addition, by shorting part or all the external front resistor, external surge voltages of shorter front duration can be made. The generators ratings are nominal voltage 1MV and rated power (energy) 7kJ. However, the actual values of surge voltages that can be produced, due to losses, are 850kV for switching impulse voltages and 885kV for lightning impulse voltages. The circuit arrangement of the generator used in the laboratory tests is shown in figure 2.6.

The process of generating the lightning impulse high voltages using the Marx generator is first carried out by supplying the generator with continuous high voltage through a test transformer and the rectifier voltage doubler, Greinacher. The test transformer, 220V/50kV, 5kVA, supplies the rectifier. The output voltage of the test transformer, which is measured using a CM type 100pF measurement capacitor through a digital voltmeter, is rectified with the help of the rectifier device which consists of two capacitors and two rectifiers.

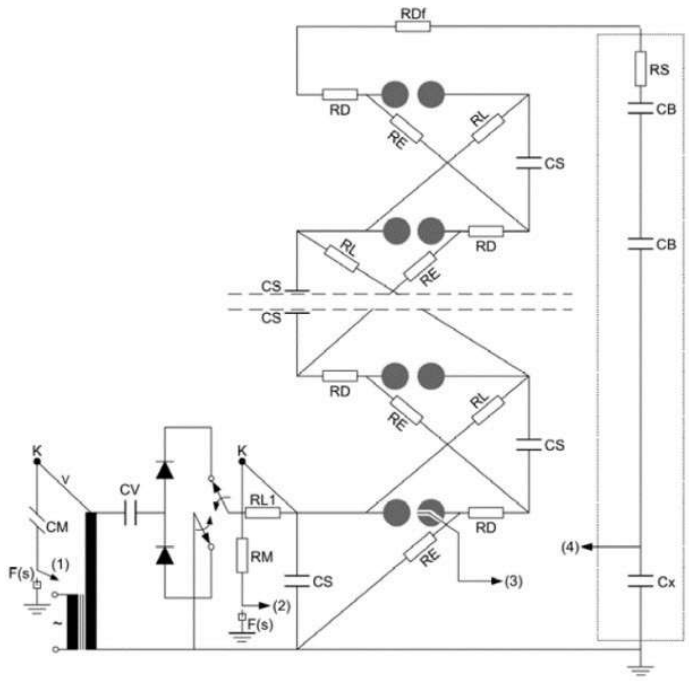

Figure 2. 6: Schematic diagram of Marx generator experimental setup

The polarity of the charging voltage depends on the direction of the rectifier diodes and the polarity reversal is carried out with the substantially reversing the diodes of the rectifier by means of a manual handle. The same capacitor (C_s) functions both as the Greinacher device's smoothing capacitor and the first-stage charging capacitor in the Marx generator. The experimental setup of the Greinacher rectifier, together with the test M/S, is shown in

figure 2.7.

The DC voltage, Vo, charges, through the charging resistor, R_{L1}, the charging capacitor of the first stage, C_{S1}. The charging capacitor of the next stage, CS2, is charged through the next charging resistor, R_{L2}, to the same potential, V_0. All ten impulse capacitors of the generator are charged in the same way. The other ends of the capacitors are grounded through the tail resistors, R_E. The actual arrangement of the Marx generator, of the high voltage laboratory of AUTH is presented in figure 2.8.

Once the high voltage pulse is applied to the auxiliary gap of the Trigatron device, the first gap, G_1, breaks down. The capacitor CS_1 is under voltage V_0 and after the breakdown of G_1 is added to the voltage of the charging capacitor of the second stage, CS_2, which is also under voltage V_0, resulting in a voltage equal to $2Vo$. Capacitors CS_1 and CS_2 are now in series. The auxiliary gap, G_2, is at $2V_0$ and breaks down almost instantaneously causing the $2V_0$ voltage to add to the voltage V_0 of the third stage capacitor, CS_3, the end of which will be at $3V_0$, as will the third stage auxiliary gap. which will break down almost instantly. The same process is repeated in all stages of the Marx generator, sequentially and almost instantaneously. Once all ten generator gaps are broken, the total voltage to ground will theoretically be $10V_0$.

The series charged capacitors discharge into the load capacitor, CB, through the front resistors, R_D, and the external front resistor, RD_f. The voltage across the load capacitor becomes equal to the output voltage of the generator. The discharge of the load capacitor is done through the front resistors, R_D, and tail resistors, R_E, as a type b circuit arrangement is used [19]. The load capacitor of the high voltage laboratory of the AUTH is shown in figure 2.9.

Figure 2. 7: Experimental setup of Greinacher

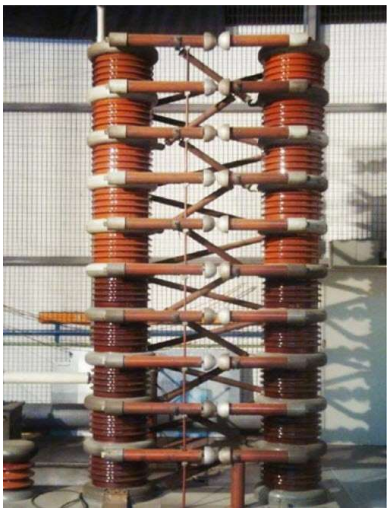

Figure 2. 8: Marx generator of the AUTH laboratory

Figure 2. 9: Load capacitor and its external resistor AUTH laboratory

2.2.2.2 Trigatron device

The ignition of the high voltage impulse generator can be either automatic or controlled. Controlled starting of the generator can be carried out by means of the Trigatron device (figure 2.10). The device combines two main electrodes that form a homogeneous field gap between them and a third auxiliary electrode that together with one of the main electrodes, usually the grounded one, forms an auxiliary gap. During operation of the device, a voltage lower than the gap breakdown voltage (DC output voltage of the Greinacher rectifier) is applied to the base electrodes. At the desired time, a high voltage pulse is imposed on the auxiliary gap. The application of the voltage pulse leads to the breakdown of the auxiliary gap and subsequently, because of the electric discharge, the

almost homogeneous field in the space of the main gap becomes locally strongly inhomogeneous and its breakdown occurs. To more precisely control the operation of the Trigatron device, the design of the auxiliary gap is changed so that when the voltage pulse is applied, the gap between the high voltage electrode and the auxiliary electrode is broken first, and then the auxiliary gap. Trigatron consists mainly of three electrodes gaps. There is a main electrode and an earthed electrode. A glass tube is positioned over the rod for this unique configuration, and it is encircled by metal foil that is connected to the primary electrode's potential. This tube's purpose is to encourage corona discharges around the rod because, in the event that a tripping impulse is delivered to the rod, this results in photoionization in the pilot gap. Primary electrons are available in the annular gap as a result of this photoionization, initiating the breakdown with little delay. The annular gap may also be filled by a glass tube (or a tube made of another solid insulating material, like epoxy resin), so that the rod and the tube's face are flush with the sphere's exterior. Thus, the tripping pulse results in a surface discharge.

Although the physical mechanism causing the major gap to break down may be fairly complex in detail, it is basically known. In fact, it is now acknowledged that there are two different kinds of active mechanisms. The distortion and increase of the electrical field between the trigger electrode and the opposite main electrode may cause a direct breakdown between these two electrodes for short spacings d and a specific tripping voltage V. For the main current, the arc then commutes from the bigger electrode to the drilled electrode. When gap distances are greater, the second kind of breakdown occurs. The annular or pilot gap breaks down due to the trigger pulse, and the main gap breaks down due to the abundance of charge carriers of all kinds that are available after sparking.

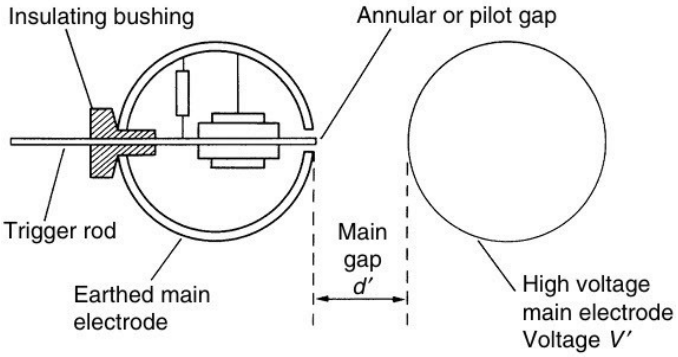

Figure 2. 10: Trigatron Spark Gap

A Trigatron device, of the MWB house, of the High Voltage Laboratory of the AUTH, is shown in Fig. 2.10. It combines a spherical gap type KF with an auxiliary electrode, an auxiliary high voltage generation device, in the form damped oscillation and a coupling capacitor. In the grounded sphere of the spherical gap is the insulated auxiliary electrode, which does not protrude from the surface of the sphere and forms with it an annular gap of 1mm. The coupling capacitor withstands the maximum charge voltage of shock capacitor.

2.2.2.3 Control desk

The control desk is type SRP 0.5/5E, rated supply voltage 220 V, 50 Hz, rated power 50 kVA, located in the measurement and test area of the main test area of the high voltage laboratory, outside the metal cage, next to the port of entry and into a shielding chamber, which is a Faraday cage. It is placed next to one of the two entrance doors of the main area of the laboratory, so that during the measurement process the splitting phenomenon is visible.

The control desk is used to control:

i. The output voltage of the autotransformer, which is used to control the output voltage of the test transformer, by means of a digital AC voltmeter.

ii. The output voltage of the Marx generator charging circuit, through a DC digital voltmeter.

iii. The Trigatron device, which is used to start the generator, allowing forvarying the distances of the auxiliary spherical gaps of the Marx generator, by means of switches and a digital indication.

Figure 2. 11: Bank of control and manipulations

In addition, it has switches for opening and closing the console, connecting and disconnecting the primary of the test transformer, and controlling the immediate power cut off safety switch. It also has instruments for measuring the supply voltage and the generated high voltages, control switches, fuses and protection relays as well as operation indicators.

2.2.3 Measurement of high impulse voltages

2.2.3.1 Digital oscilloscope- current transformer-signal attenuator

A LeCroy WR64Xi oscilloscope was used to visualize and measure the high voltage surge waveforms during the experimental process, as well as to determine the breakdown time, breakdown voltage, current and other measurements. The bandwidth of this oscilloscope is 600 MHz, and the sampling frequency is 5 Gs/s. The oscilloscope was connected to the low voltage side of the capacitive voltage divider, high voltage capacitance of the load capacitor of the Marx generator, 200pF and low voltage capacitance of 0.296μF.

Figure 2. 12: Digital Oscilloscope

To record and measure the current signal, a current transformer of the PEARSON company type 301X, 0.01 Volts per Amp and a signal attenuator of the PEARSON company type A10, 10:1 Voltage Ratio is used. The device's grounding cable passes through the current transformer, while the output of the transformer is connected to the oscilloscope through the signal attenuator. Using the two devices helps to downscale the signal by a factor of 1 to 1000 so that the current waveform can be displayed on the oscilloscope.

Figure 2. 13: PEARSON 301X Current Transformer and Signal Attenuator PEARSON Attenuator A10

The connection of the digital oscilloscope to the capacitive voltage divider was carried out using a coaxial cable with a grounded jacket, shielded against electromagnetic noise by means of a metal jacket. In the same way, the connection of the transformer was carried out, through the signal attenuator. The digital oscilloscope operates within a shielding cage which is connected to the earthing facility of the main test room of the high voltage laboratory through the earthed sheath surrounding the coaxial cable. In this way, closed earth loops between the coaxial cable and the earthing system are avoided.

2.2.4 Essays

In the context of this diploma work, the phenomenon of the electrical flashover of the insulating tube supporting the air termination was studied. Experiments were carried out on three different insulating tubes differing in material and geometry. For each category of the above gaps, measurements were made with imposed lightning impulse high voltages of 1.1/50μs positive and negative polarity.

Tube 1 and tube 2 are of same geometry but differ in material. Similarly, tube 2 and tube 3 are of same material but has different geometry. Tube 3 has an addition layer on the top and bottom of the tube.

Figure 2. 14*:* Material under study

2.3 Equipment

In summary, the equipment used during the experimental process, both for the generation of the impulse high voltages and for the control and display measurement of quantities at the entrance and exit of the Marx generator, are SRP type SRP 0.5/5E construction control bank, V/m peak type SM76 and continuous type GM78, one measuring resistor type R_M 280MΩ, 140kV, one R_E type resistor 282kΩ, 60W, 140kV. Marx ten-stage generator 1MV/ 7kJ of the house Ferranti which combines the following elements: M/S test 2×220V/50 kV, 5kVA, 4%. Capacitor, C_V, 25nF, 100kV, ten shock capacitors, C_S, 0.14μF, 100kV,two load capacitors, C_B, 400pF, 450kV,eight load resistors, R_L , 56.5kΩ, 100kV,two load resistors, R_L, 19.7kΩ, 100kV,ten tail resistors, R_E, 500Ω, 100kV, ten front resistors, R_D, 35Ω, 100kV, front resistance, R_{Df}, RD_f of 1Ω for 0.34/7μs waveform, RD_f of 1257.33Ω for 1.1/50μs waveform ,damping resistor R_S 100Ω, low voltage branch of capacitive voltage divider combining 0.29 μF capacitor and 75 Ω matching resistor was also used. LeCroy WR64Xi type digital oscilloscope, PEARSON 301X Voltage Transformer, Volts per Amp 0.01, PEARSON A10 Voltage Ratio 10:1 signal attenuator was used for the measurement process.

2.4 Experimental Setup

As already stated, the complete circuit required for high voltage equipment testing consists of the high voltage generator, the connection to the test specimen, the test specimen itself and finally the voltage and current measurement systems. For the experimental device used in the context of this thesis, the role of the high voltage production device is assumed by the Marx generator. The capacitor of this front performs a double function, i.e. it also serves as a high voltage capacitor of the capacitive divider. The generated impulse voltage is transferred from the Marx output to the tip of the air termination 1 m height. Figure 2.15 shows the layout for the experiment setup.

Figures 2.15 and 2.16 show the two arrangements as photographed during the experiments.

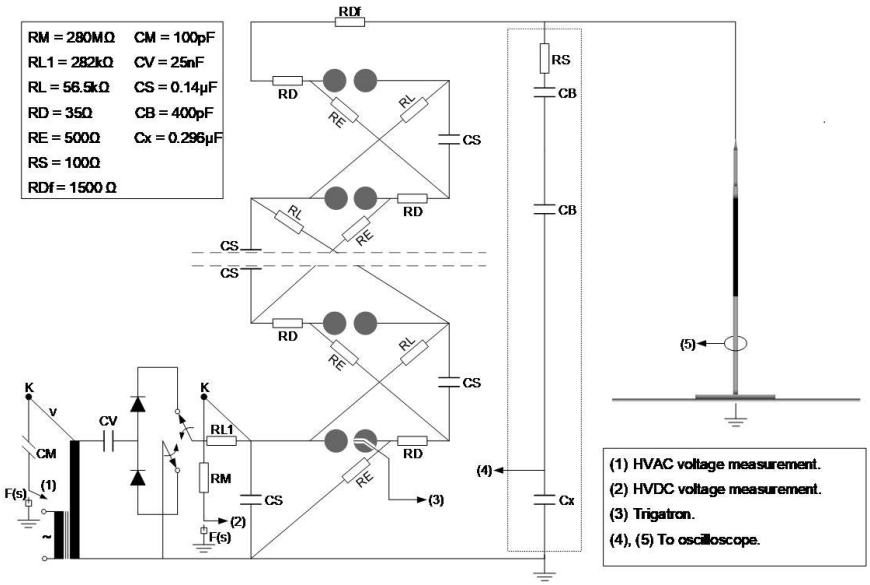

Figure 2. 15:Overall layout for experiment

Figure 2. 16: Air termination under test

The devices are grounded through a suitable cable that passes through the voltage transformer for current measurement purposes (figure 2.17, 2.18) and end at the grounded floor. The output of the current transformer ends up via a suitably shielded cable to the signal attenuator which is connected to the oscilloscope.

Figure 2. 17: Overall experimental setup

Figure 2. 18: Current measurement through a current transformer

CHAPTER THREE: SIMULATION INVESTIGATION OF ELECTRIC FIELD USING COMSOL

To investigate the electric field potential for all insulating tubes, the model is developed in COMSOL. Figure 3.1 shows the 3D modeling for tube 1 and 2 as they have the same geometry and differ only in material. The permittivity is set as 2.3. Calculating internal and external flashovers in insulating tubes within lightning protection systems is essential to ensure the system's safety and reliability. Internal flashover occurs when the electric field exceeds the dielectric strength of the insulating material, potentially causing insulation failure, while external flashover happens when the surface electric field surpasses the breakdown strength, leading to arcing. In COMSOL, these calculations help predict and prevent flashovers, allowing for optimized tube design, material selection, and system performance. By evaluating these factors, you can avoid system failure, ensure safe routes of lightning currents, and maintain the integrity of the protection system.

Figure 3. 1: 3D design on COMSOL for IT 1

Figure 3. 2: 3D design on COMSOL for IT3

The electric potential is applied on the tip of the air termination. The base of the air termination is grounded as shown in figure 3.5-3.6. The tip and the base as of steel. Figure 3.3 shows the electric potential distribution of insulating tube.

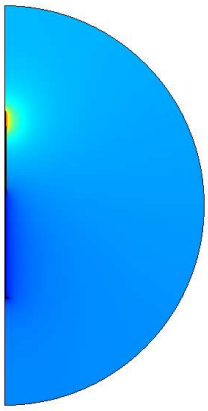

Figure 3. 3: Electric potential distribution of insulating tube 1

The 3D model was converted to 2D Axis symmetric model as it is more simplified and less time-consuming. The air termination was stressed with voltage whereas the base was ground. The electric field distribution both internal as well as external was simulated.

Figure 3. 4: 2D model for insulating tube

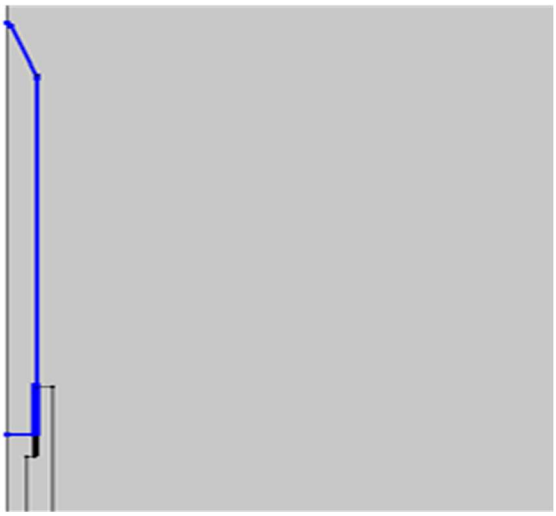

Figure 3. 5: 3D design on COMSOL for IT1

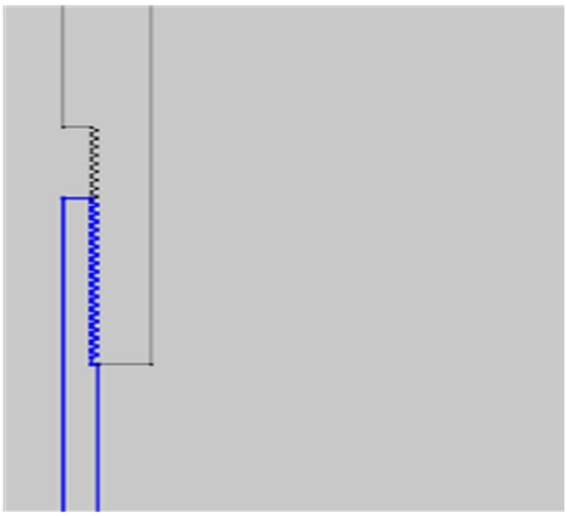

Figure 3. 6: 3D design on COMSOL for IT 1

The figures 3.7-3.8 show the electric field distribution for insulating tube 1. X-axis shows the arc length (cm) and Y-axis shows the electric field V/(m.V)

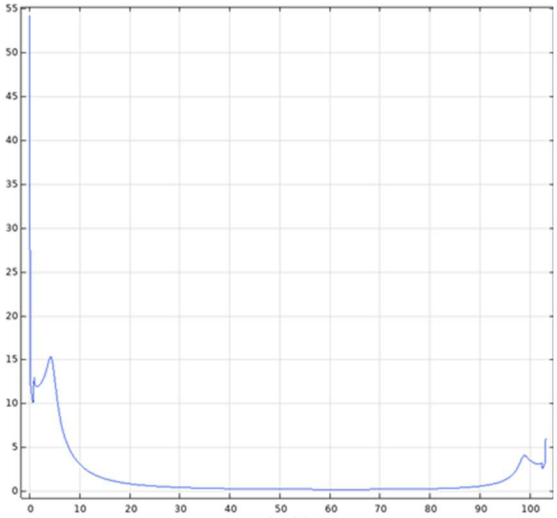

Figure 3. 7: External electric field vs arc length

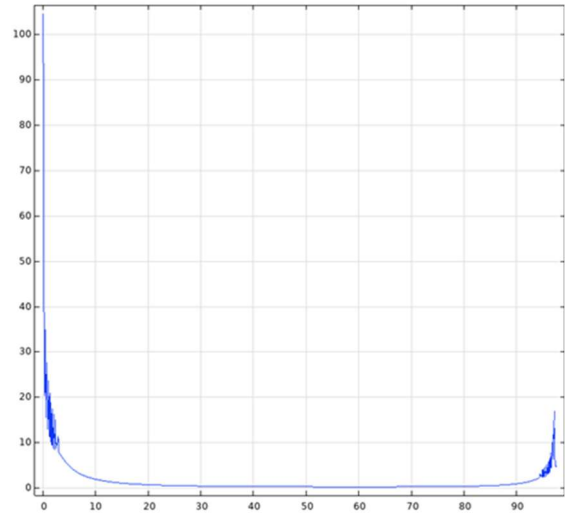

Figure 3. 8: Internal electric field vs arc length

The figures 3.9-3.10 show the electric field distribution for insulating tube 3. X-axis shows the arc length (cm) and Y-axis shows the electric field V/(m.V)

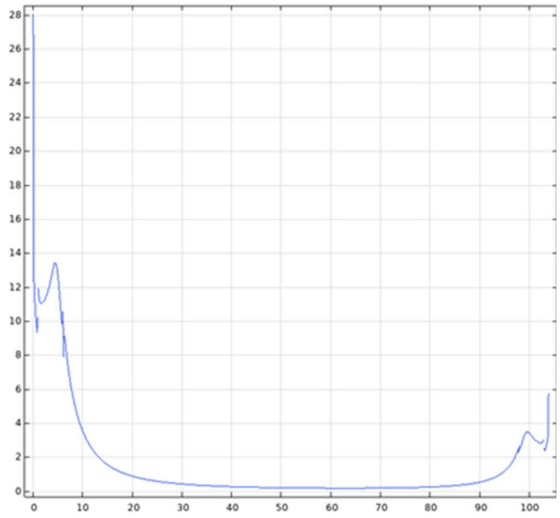

Figure 3. 9: External electric field vs arc length

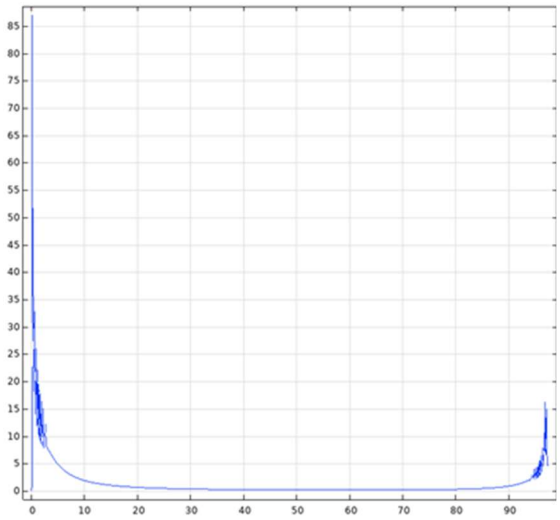

Figure 3. 10: Internal electric field vs arc length

From the electric field distribution, it is seen that the electric field is less in tube 3 than tube 2. It is because of the additional layer on the top and bottom of the insulating tube 3. The initial on the graph is the striking point i.e. air termination and the electric field goes on decreasing as it passes through the insulating tube and again sharply increases when it reaches the base which is conducting.

In both the cases, it is seen that the internal electric field is greater than the external electric field which says that the flashover is more probable to be from internal surface rather than the external surface which is also supported by the experiment. The change in the permittivity and the respected internal and external electric field for tube 1 and tube 3 was simulated.

Table 3. 1: Effect of permittivity on electric field for Tube 1/2

TUBE 1/2				
Relative permittivity	External electirc field	Internal electric field	% change in external electric field	% change in internal electric field
2	56.655	107.8327	1.43	1.02
2.1	55.845	106.7286	1.44	1.02
2.2	55.038	105.6357	1.45	1.03
2.3	54.238	104.5464	1.46	1.03
2.4	53.447	103.469	1.46	1.03
2.5	52.665	102.4058	1.46	1.02
2.6	51.898	101.3565	1.45	1.02
2.7	51.14	100.3263	1.44	1.01
2.8	50.4	99.3146	1.45	1
2.9	49.67	98.321	1.44	0.99
3	48.955	97.347		

Table 3. 2: Effect of permittivity on electric field for Tube 3

TUBE 3				
Relative permittivity	External electric field	Internal electric field	% change in external electric field	% change in internal electric field
2	29.613	91.5698	1.83	1.72
2.1	29.073	89.9937	1.81	1.69
2.2	28.548	88.4747	1.79	1.66
2.3	28.0366	87.0096	1.77	1.62
2.4	27.5403	85.5987	1.75	1.59
2.5	27.057	84.238	1.73	1.56
2.6	26.588	82.9277	1.71	1.52
2.7	26.133	81.663	1.69	1.49
2.8	25.6902	80.443	1.67	1.46
2.9	25.26	79.268	1.66	1.43
3	24.842	78.133		

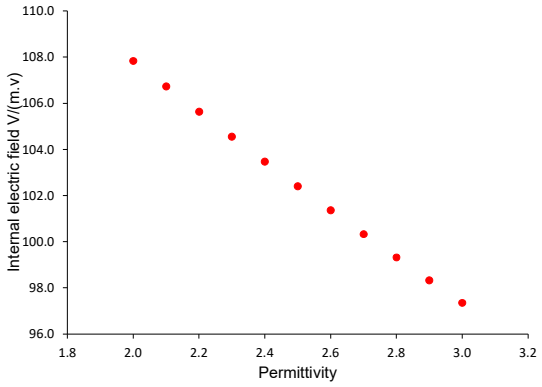

Figure 3. 11: Permittivity vs internal electric field (IT1)

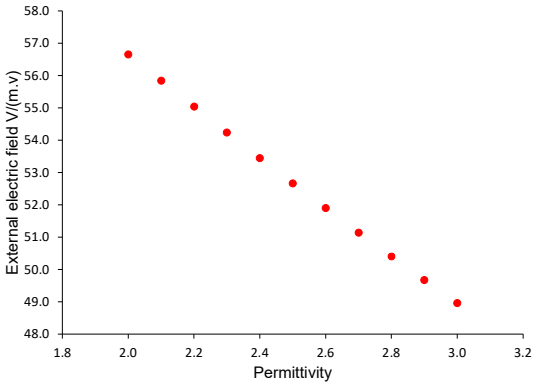

Figure 3. 12: Permittivity vs external electric field (IT1)

Permittivity is a measure of how easily a material can be polarized by an electric field.

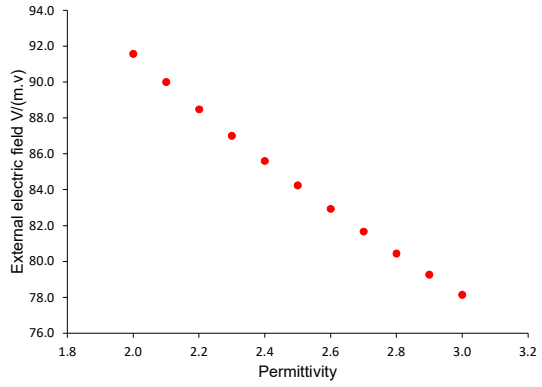

Figure 3. 13: Permittivity Vs internal electric field (IT3)

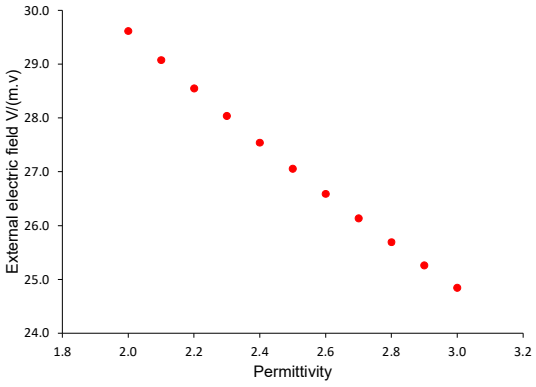

Figure 3. 14: Permittivity Vs external field (IT3)

When the permittivity increases, the material becomes more polarizable, meaning that the

charges within the material (electrons and nuclei) can realign themselves more easily in response to an external electric field. As the permittivity increases, the withstand capacity of the insulating tube is also increased as the electric field is decreased.

CHAPTER FOUR: MEASUREMENT PROCEDURE

This chapter presents the basic definitions of the experimentally measured in order to assess the dielectric strength and flashover characteristics of insulating tubes. Finally, the measurement standards are presented in detail, i.e. the way in which the measurements were taken during the preparation of the experiments [1].

4.1 Basic definitions

4.1.1 50% breakdown voltage, U_{50}

Breakdown voltage U_{50} is defined as the value of the imposed stress for which the probability of breakdown is 50% [1], i.e. a certain number of impositions under the specific stress leads to a 50% probability of breakdown and a 50% probability of strength.

4.1.2 Flashover voltage (U_p)

The flashover voltage is defined as the voltage at which the electrical flashover of an insulation occurs [1]. Its value is mainly determined by the mechanism of electrical discharge, from the moment of application of the stress voltage to the moment of flashover. In this work, flashover voltage, U_p, was defined as the maximum voltage stressing the insulating stand-offs until flashover, and in fact it is the voltage which eventually causes flashover.

4.1.3 Time to flashover (t_f)

The flashover time is conventionally defined as the time interval between the application of the stress and its collapse [1]. This definition is used if no current measurements are performed. In this thesis due to the current measurements, the time at which the maximum current occurs was defined as the time to flashover. At flashover, the spark channel is assumed to bridge the entire gap.

4.1.4 Maximum current value (I_p)

The maximum spark current value or peak current was defined at the time instant when the current value is maximum, at the peak of the waveform.

3.1.5 Applied voltage (U_{app})

The applied voltage, U_{ap}, is obtained if the loading voltage of the first stage of the Marx generator is multiplied by the number of stages of the generator, n, and by the measured utilization factor of the generator, n.

4.1.6 Voltage at maximum current value (UI_p)

The voltage at the maximum value of the current, is defined as the value of the voltage at the time instant of maximum current, i.e. at the time defined as the flashover time.

4.2 Experimentally obtained curves

4.2.1 Flashover Probability-Flashover probability curves

Because of the stochastic nature of the electrical breakdown phenomenon, the breakdown voltage is subject to statistical variation and usually requires a series of tests to determine it with statistical reliability. The breakdown probability is defined as the probability that the application of a voltage of a certain type and value will cause the electrical breakdown of the insulation.

If the breakdown probability is assumed to depend only on the value of the applied stress, the dielectric behavior of an insulation can be estimated through the breakdown probability distribution, P(U), which relates the resulting pairs of values of applied stress and breakdown probability experimentally by varying the applied voltage. The breakdown probability distribution can be analytically defined as a function of the 50% breakdown voltage, U_{50}, which is the value of the voltage for which the breakdown probability is 50%, and the conventional deviation, z, which is calculated as the difference $U_{50} - U_{16}$, where U_{16} is the voltage value for which the probability of breakdown is 16%.

The normal distribution can typically provide a satisfactory approximation of the breakdown probability distribution - Gaussian - and therefore the experimental data satisfy the cumulative distribution of Equation according to Kuffel in [13].

$$P(U) = \frac{1}{z\sqrt{2\pi}} \int_{-\infty}^{U} \exp\left(-\frac{(U - U_{50})^2}{2z^2}\right) \tag{4.1}$$

Breakdown stress U_{50} is defined as the value of the imposed stress for which the probability

of breakdown is 50%, i.e. for a certain number of impositions under the specific stress we are led to a 50% probability of breakdown and a 50% probability of strength.

4.2.2 Flashover voltage-time to flashover characteristics (U_p-t_f)

Depending on the amplitude of the applied voltage, flashover occurs either during the wavefront or the wave tail of the applied impulse voltage. The voltage-time characteristic, is a graph which, for a series of voltage levels, plots either the instantaneous value or the maximum value of each level as a function of the corresponding decay time, depending on whether it occurs at the front or the tail of the applied voltage A time-voltage characteristic curve is shown in Figure 4.1 [17]. An essential practical feature of every insulating construction or device, including insulators, is the characteristic voltage-time curve. It offers the foundation for figuring out how well an area is protected from overvoltage.

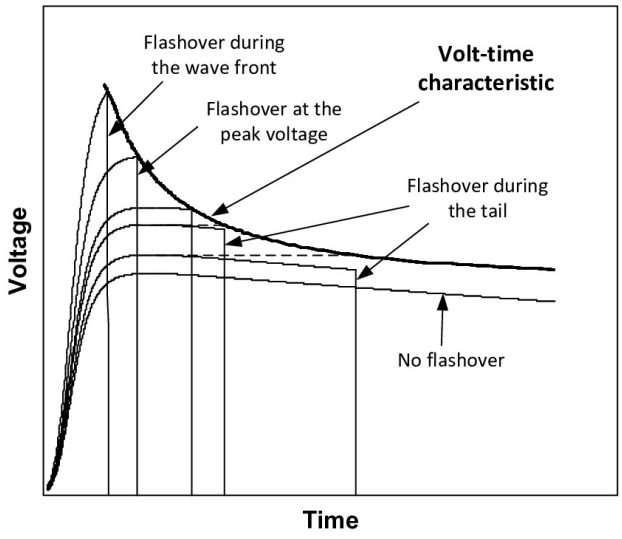

Figure 4. 1: Flashover voltage-time to flashover curve

4.2.3 Maximum current-flashover voltage (I_p-U_p)

The I_p-U_p curves present the maximum current as a function of the flashover voltage. The purpose of deriving these curves is to study the current that results for each flashover voltage, current which is a result of this voltage.

4.2.4 Spark conductance based on flashover voltage vs applied voltage (I_p/U_p-U_{ap})

The I_p /U_p -U_{ap} curves show the spark conductance based on the flashover voltage as a function of the amplitude of the applied voltage.

4.3 Multiple levels method

The stochastic nature of the flashover phenomenon results in the statistical variation of the breakdown voltage. Therefore, the reliable determination of the flashover voltage is carried out through statistical analysis of the test results. There are three methods of determining the flashover voltage, the multiple levels method, the up and down method and the sequential breakdown method. In this thesis, to determine the surface flashover voltage of the standoffs, the multiple levels method is used.

In applying the method, a voltage of constant value, (voltage level) is imposed on the insulation several times at each of the voltage levels. From the ratio of the number of flashovers observed, to the number of impositions, of the voltage per level, the flashover probability is obtained.

When applying the method, a constant value voltage, U_i (voltage level U_i) is imposed on the insulation m times at each of the n voltage levels. From the ratio of the number of decays observed, di, to the number of impositions, m, of the trend per level, the probability of breakdown per level is derived from equation [13].

$$P(U_i) = \frac{d_i}{m} \tag{4.2}$$

4.4 Impulse voltage waveforms

These waveforms, as extracted from the measurement processing, are shown in Figure below.

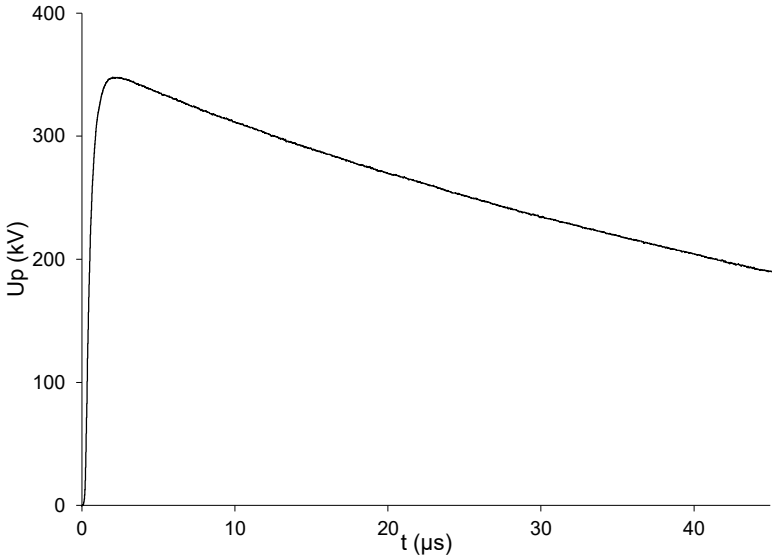

Figure 4. 2: Imposed voltage waveform (+)

4.5 Measurement standards

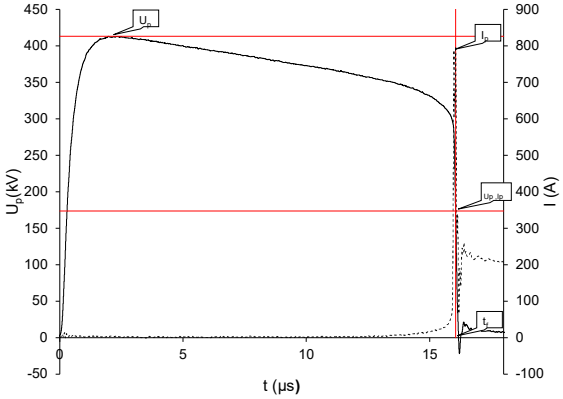

Figure 4. 3: V-T curve at lower voltage breakdown

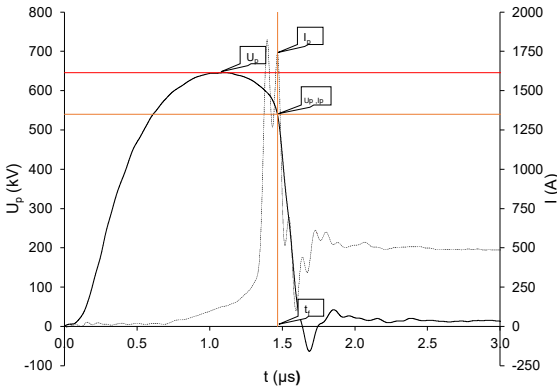

Figure 4. 4: V-T curve at higher voltage breakdown

Flashover characteristics of insulating tube were investigated under standard lightning impulse voltage of both positive and negative polarity. In case of negative polarity for insulating tube 3 a different approach was followed. Lightning impulse voltages of relatively high and gradual increasing amplitude was initially applied. After the first flashover, repetitive flashovers were observed. The reduced lightning impulse voltage was then applied. The procedure was repeated using multiple level tests.

CHAPTER FIVE: EXPERIMENTAL RESULTS

In this chapter, the diagrams extracted from the processing of the experimental data are presented, the results are commented on, and conclusions are drawn regarding the effect of the factors considered, the polarity and the types of insulating tubes. The measurements taken concern the flashover voltage and time, the instantaneous flashover voltage (voltage at maximum discharge current) and the peak discharge current. The results are commented, and conclusions are drawn regarding the effect of the amplitude and polarity of applied voltage and the geometry of the insulating tubes on flashover characteristics.

5.1 Breakdown probability curves

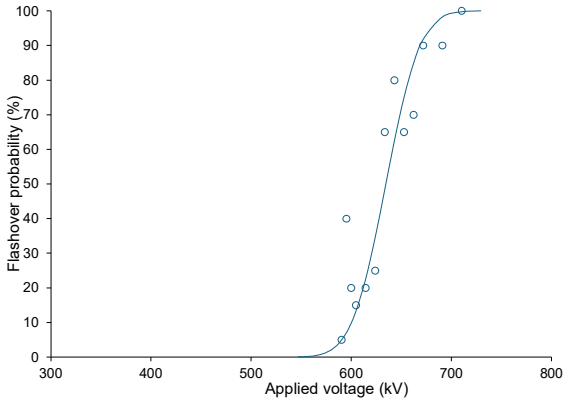

Figure 5. 1 Breakdown probability curve for IT 1(+)

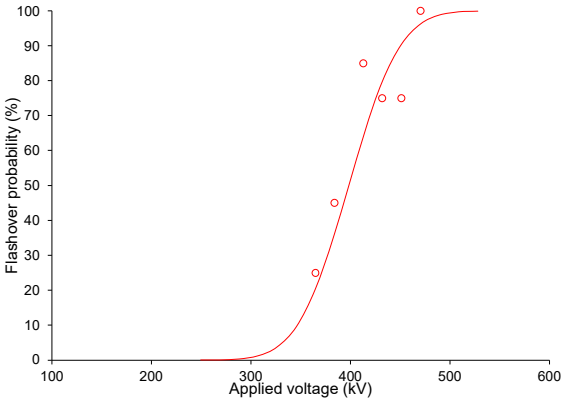

Figure 5. 2: Breakdown probability curve for IT1 (-)

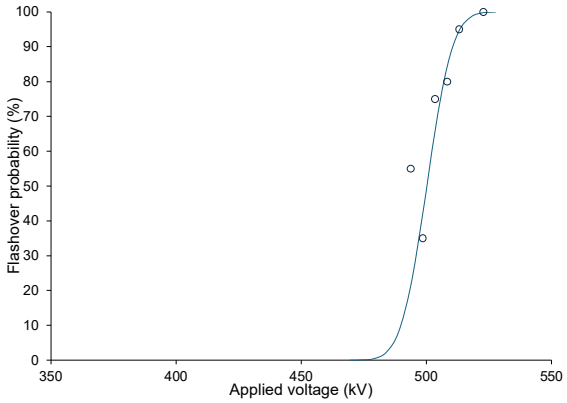

Figure 5. 3: Breakdown probability curve for IT 2 (+)

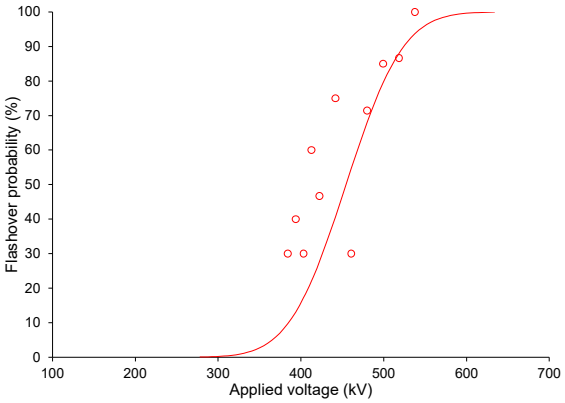

Figure 5. 4: Breakdown probability curve for IT 2 (-)

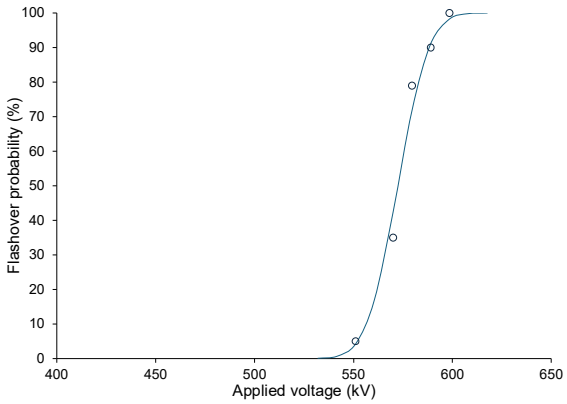

Figure 5. 5: Breakdown probability curve for IT 3 (+)

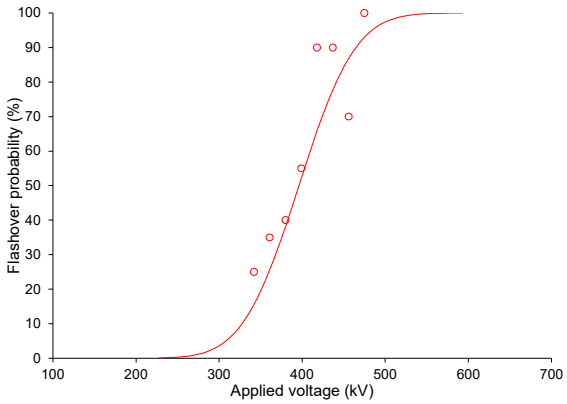

Figure 5. 6: Breakdown probability curve for IT 3 (-)

Based on the experimental results, the flashover probability curves and their approximation with the normal distribution were constructed. The breakdown probability for all tubes for positive and negative polarity are shown in figures 5.1-5.6.

Listed below in Table 1 for each arrangement are the values of the 50% flashover voltage (U_{50}), standard deviation σ (%) as well as the corresponding atmospheric conditions for both positive and negative polarity.

Table 5. 1: Aggregate results of 1.1/50 μs waveform

	Polarity	P (mmHg)	T (°C)	H (gr/m^3)	δ	σ (%)	U_{50} (kV)
Tube-1	+	760.5	16	10.33	1.0145	4.23	634.68
	-	762	18	12.1	1.0095	10.16	398.4
Tube-2	+	765	16	11.3	1.0205	1.61	500.2
	-	765	16.5	12.23	1.0187	11.94	454.56
Tube-3	+	768	17	11.96	1.0210	2.16	572.38
	-	765	17.5	11.72	1.0152	13.5	396.15

5.1.1 Effect of polarity on flashover probability curve

In this section the effect of the polarity of the applied voltage on the flashover probability curves is considered. Thus, the flashover probability curves were drawn in a common diagram for both polarities shown in the figures 5.7-5.9.

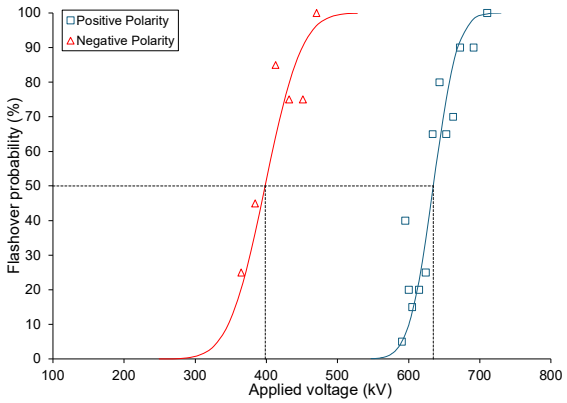

Figure 5. 7: Breakdown Probability curve IT 1

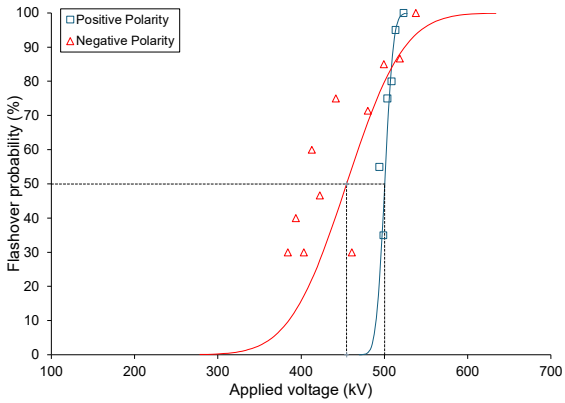

Figure 5. 8: Breakdown probability curve for IT 2

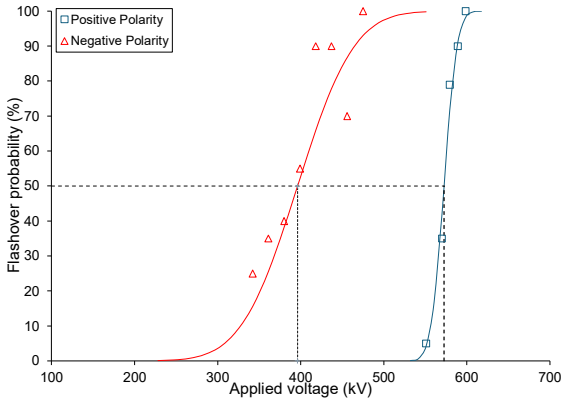

Figure 5. 9: Breakdown Probability curve for IT 3

From the above figures, it is observed that the breakdown probability curve for positive polarity is to the right to the corresponding one for positive polarity, i.e. U_{50} is greater for positive polarity. A higher U_{50} for positive polarity indicates that the material or system can withstand a greater positive voltage before breakdown occurs compared to the negative voltage. Positive lightning strikes typically involve a more gradual buildup of charge and a less intense electric field near the air termination system. This slower development gives the insulating tube more time to resist breakdown, resulting in a higher U_{50}. Negative lightning often involves a rapid increase in electric field intensity and electron avalanche formation. This rapid ionization reduces the U_{50} for negative polarity. In positive polarity, corona discharge occurs more gradually because the ionization of air around the insulating tube is less intense. This helps delay the onset of breakdown, increasing U_{50}. Negative polarity can create localized charge accumulations (space charges) at the insulating tube.

These charges distort the electric field and increase the likelihood of premature breakdown, lowering U_{50}. The greater U_{50} for positive polarity in an insulating tube within an air termination system for a lightning protection system arises from the differences in electric field dynamics, ionization behavior, and surface interactions with the discharge. It seems that positive polarity leads to smoother, less intense ionization processes and slower streamer propagation, allowing the system to withstand higher voltages before breakdown occurs.

5.1.2 Effect of materials on breakdown probability curve

The tube 1 and tube 2 has the same dimension and geometry but differ only on the material of the insulating tube. Figure 5.10-5.11 shows the effect of material on the flashover probability curve.

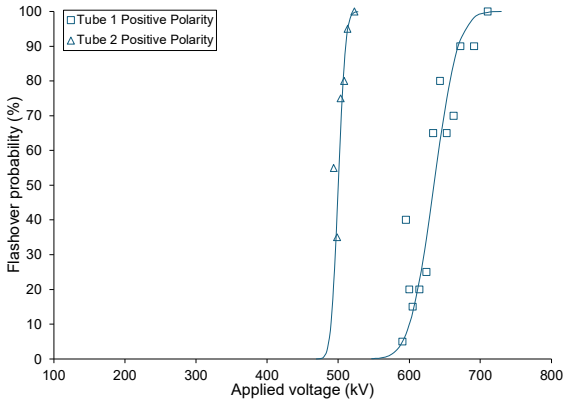

Figure 5. 10: Breakdown curve for IT 1 and 2 (+)

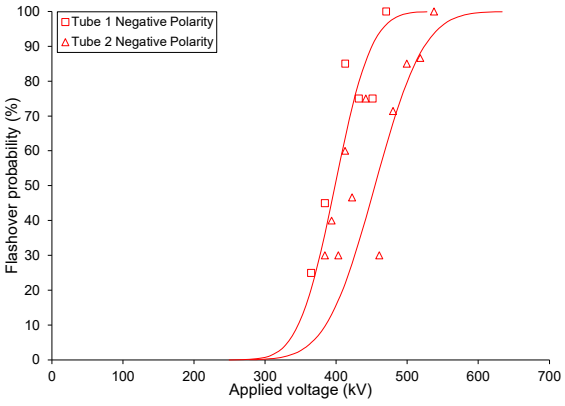

Figure 5. 11: Breakdown curve for IT 1 and 2 (-)

The U_{50} of an insulating material depends on the polarity of the applied voltage which is known as polarity effect. This mainly arises due to the difference in how the electrons and ions interact with material under positive and negative polarity. In case of positive polarity, electrons are emitted from cathode and accelerated towards anode where negative polarity involves positive ions or holes with interact with the material in a different way.

In case of positive polarity, the tube 1 has higher U_5 than of tube 2. But in the case of negative polarity, the tube 1 has lower U_{50} than in case of tube 2.

The insulating material used for tube 1 has higher work function or better electron emission

suppression under positive polarity which leads to higher U_{50}. Similarly, tube 2 is more prone to electron emission reducing the U_{50}. The mobility of positive ions in the material for tube 1 and 2 differ. Tube 2 allows for easier movement of positive ions under negative polarity, increasing U_{50} compared to tube 1.

Hence the differences in U_{50} are primarily due to the material's inherent properties and how they interact with charge carriers under different polarities. So, each material has unique advantages and disadvantages depending on the applied voltage polarity.

5.1.3 Effect of geometry on breakdown probability curve

The insulating tube 2 and 3 are made up of same material but they differ in the dimension. The tube 3 has an addition layer of insulating on the top and bottom of the tube. Figure 5.12-5.13 shows the effect of geometry on the flashover probability curve.

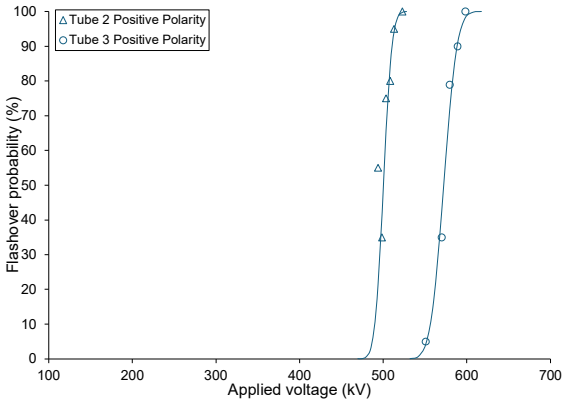

Figure 5. 12: Breakdown curve for IT 2 and 3 (+)

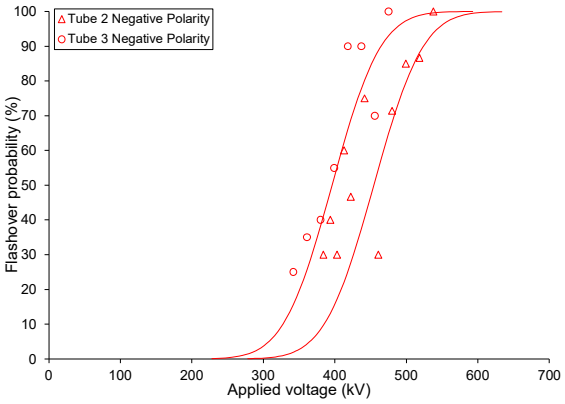

Figure 5. 13: Breakdown curve for IT 2 and 3 (-)

In case of positive polarity, tube 2 has lower U_{50} than tube 3. For tube 2 it has lower breakdown voltage because it has no additional insulating layer, making it more susceptible to breakdown under high electric fields. For tube 3, it has higher breakdown voltage because the additional insulating layer increases the overall insulation strength making it harder for breakdown to occur.

In case of negative polarity, U_{50} of tube 2 is higher than that of tube 3. Tube 2 has higher breakdown voltage because the single insulating material behaves more uniformly under negative bias. Tube 3 has lower breakdown voltage because the additional insulating layer

may introduce interface defects or charge trapping sites at the boundaries between the layers. These defects enhance local electric fields, making breakdown easier under negative polarity.

5.1.4 Effect of all samples on breakdown probability curve

The flashover probability curves of insulating tube differing are plotted in Figure 5.14-5.15 to show the effect of material and dimension on the flashover probability curve.

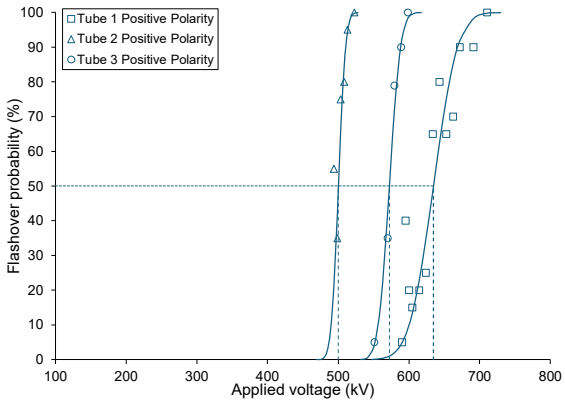

Figure 5. 14: Breakdown curve for IT 1,2 and 3 (+)

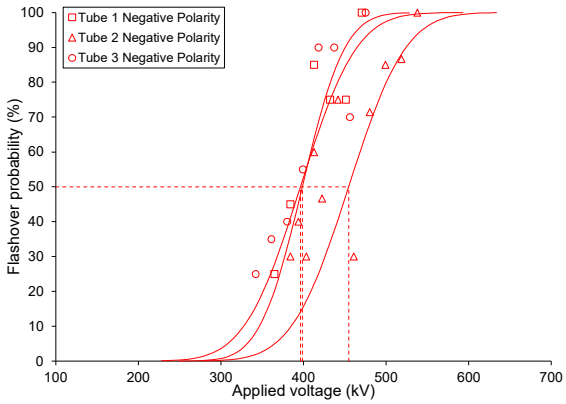

Figure 5. 15: Breakdown curve for IT 1,2 and 3 (-)

In case of positive polarity, tube 1 has the highest U_{50} (634.68 kV) with the highest standard deviation followed by tube 3 (572.38 kV) and tube 2 (500.2 kV). As tube 1 and tube 2 have the same dimension but differ in material, it is seen that the material of tube 1 can withstands more than that on the tube 2. Similarly, tube 2 and tube 3 have the same material but they differ in geometry, tube 3 can withstand a bit more than that of the tube 2 (as it has additional insulation on either side of the tube). In case of negative polarity, tube 2 has the highest U_{50} (454.56 kV) followed by tube 3 (396.15 kV) and tube 1 (398.4 kV). It suggested that the material for tube 2 and 3 have greater dielectric strength and can withstand more than that of tube 1. So, tube 1 is more resistant to lightning for positive polarity and tube 2 is more resistant to lightning for negative polarity.

5.2 Maximum flashover current-voltage curves (I_p-U_p)

The I_p-U_p curves were constructed to enable the study of the resulting discharge current as

a function of the flashover voltage. The general conclusion drawn from diagrams 5.16-5.21 is, as expected, the discharge current increases with the increasing applied voltage. It is observed that the increment of the discharge current is proportional to the flashover voltage.

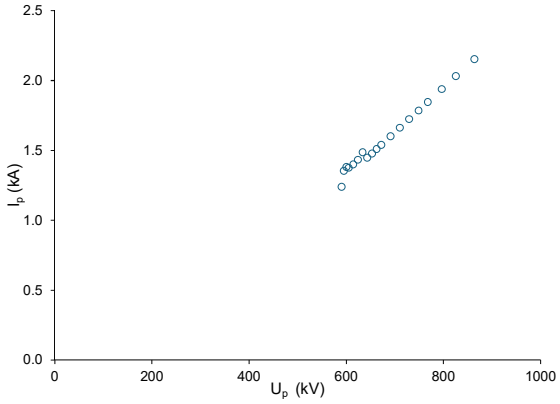

Figure 5. 16: I_p-U_p curves for IT 1 (+)

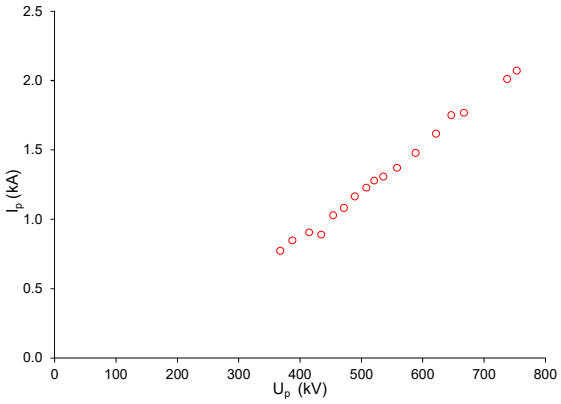

Figure 5. 17: I_p-U_p curves for IT 1 (-)

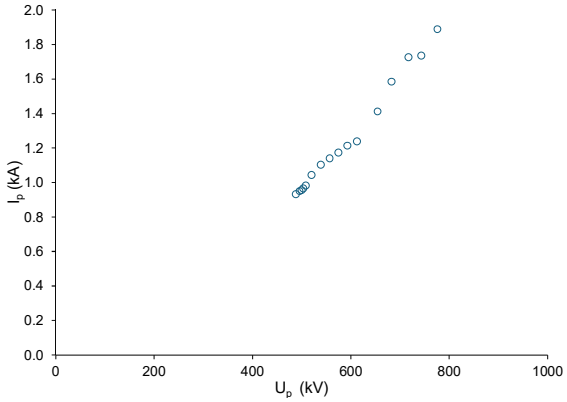

Figure 5. 18: I_p-U_p curves for IT 2 (+)

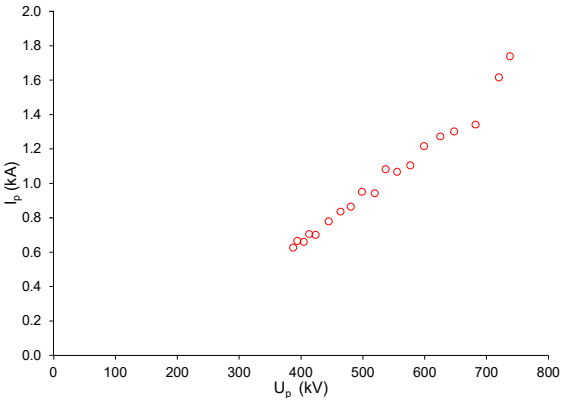

Figure 5. 19: I_p-U_p curves for IT 2 (-)

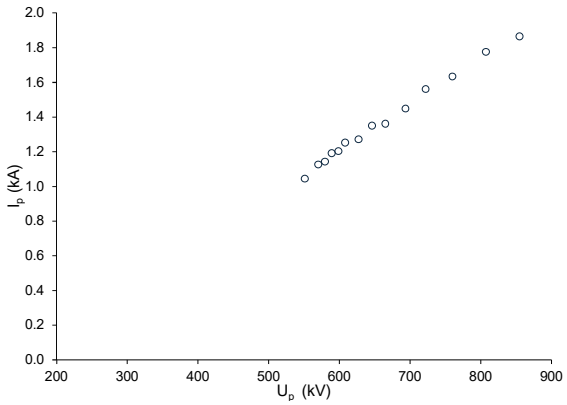

Figure 5. 20: I_p-U_p curves for IT 3 (+)

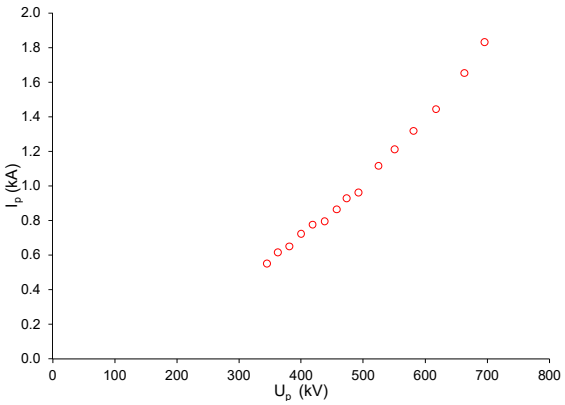

Figure 5. 21: I_p-U_p curves for IT 3 (-)

5.2.1 Effect of polarity on I_p-U_p curves

The effect of polarity of the applied voltage on I_p-U_p curves in figures 5.22-5.24. It can be observed that the discharge current is generally higher under negative than the positive polarity impulses, with the effect being similar for all the insulating tubes. Generally, with increasing applied voltage the discharge current increases linearly with flashover voltage.

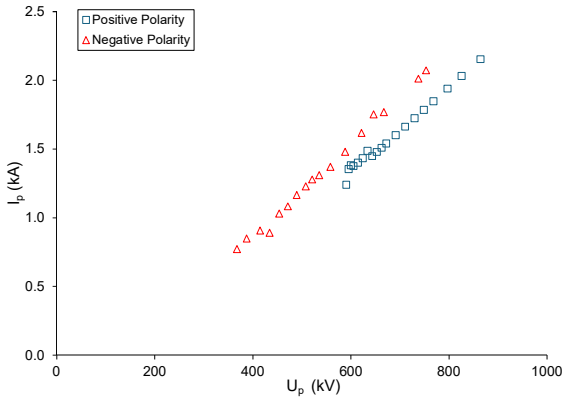

Figure 5. 22: I_p-U_p curves for IT 1

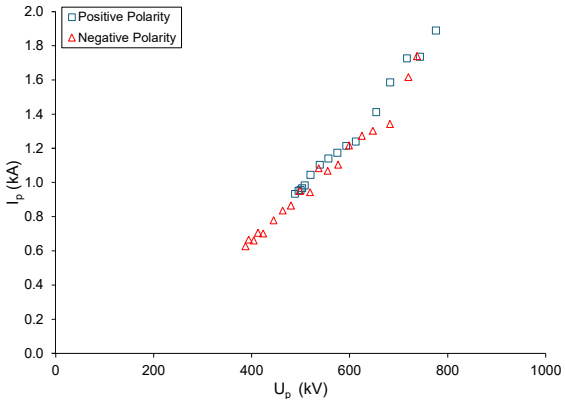

Figure 5. 23: I_p-U_p curves for IT 2

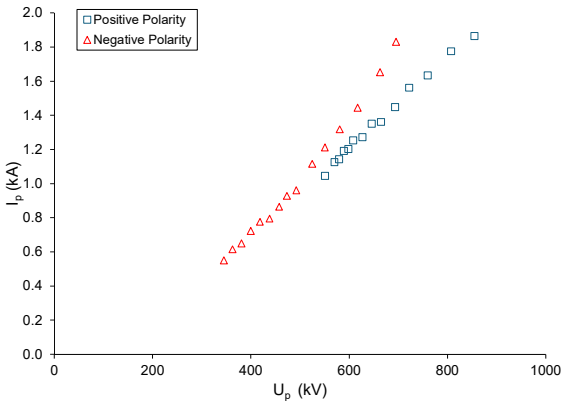

Figure 5. 24: Figure 5.24: I_p-U_p curves for IT 3

5.2.2 Effect of material on I_p-U_p curves

In this section the effect of the material on insulating tube on the I_p-U_p are shown in figures 5.25-5.26.

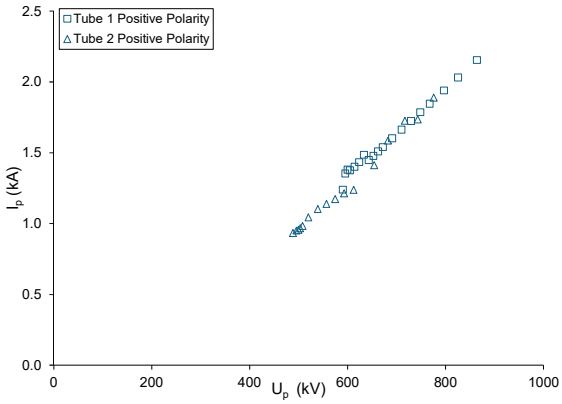

Figure 5. 25: I_p-U_p curves for IT 1 and 2 (+)

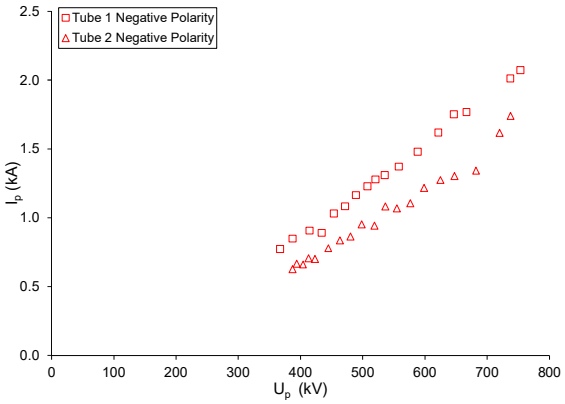

Figure 5. 26: I_p-U_p curves for IT 1 and 2 (-)

The I_p-U_p curve for tube 1 and tube 2 shows a similar behavior. Under positive polarity, the flashover process is primarily driver by electron emission from cathode and formation of conductive plasma channel. The similar curve for positive polarity suggests that the electron emission characteristics and the plasma formation process are comparable for both materials under positive polarity.

The U_{50} is different in case of positive polarity but the I_p-U_p curve is similar for positive polarity. This is because once the breakdown is initiated, the flashover process (formation

and propagation of the plasma channel) might be governed by similar mechanisms in both materials. After the initiation of breakdown, the flashover process is influenced by factors like gas ionization, surface conductivity, and plasma propagation which indicated to be similar for both the material.

Tube 1 is more susceptible to breakdown initiation than tube 1 under negative polarity. However, the higher maximum flashover current-voltage curve for tube 1 indicates than once the breakdown occurs, the flashover in tube 1 involves higher current or energy dissipation compared to tube 2. Under negative polarity, tube 1 material have lower resistance to surface charge making it easier for breakdown to lower U_{50}.

5.2.3 Effect of geometry on I_p-U_p curve

In this section the effect of the geometry on insulating tube on the I_p-U_p are shown in figures 5.27-5.28.

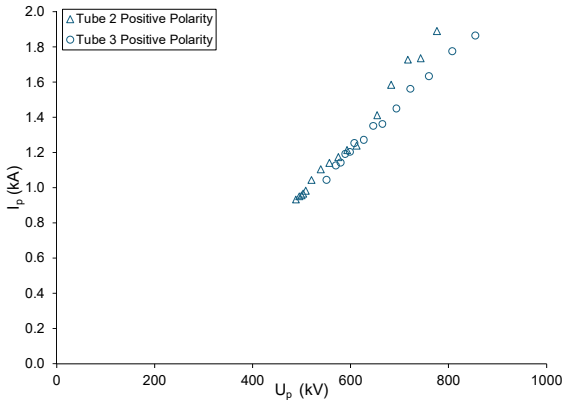

Figure 5. 27: I_p-U_p curves for IT 2 and 3 (+)

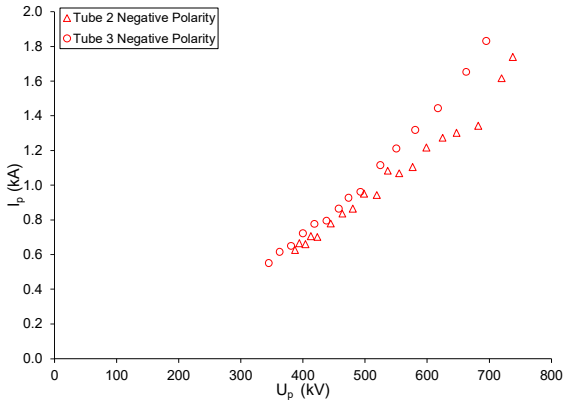

Figure 5. 28: I_p-U_p curves for IT 2 and 3 (-)

Tube 2 and tube 3 has similar maximum flashover current-voltage curve as under positive polarity, the electric filed distribution is more uniform, and the additional insulating layer in tube 3 does not significantly alter the overall behavior. The flashover process is dominated by the bulk properties of the insulating material, which are the same for both tubes. The additional layer in tube 3 does not introduce significant defects or non-uniformities that would affect the flashover process under positive polarity.

Under negative polarity, the additional insulating layer in tube 3 introduces interface effects

(eg charge trapping, defects, or enhanced local electric fields) at the boundaries between layers. These interfaces can act as sources of secondary electron emission or field enhancement sites which can sustain a higher flashover current once the breakdown process is initiated.

5.2.4 Effect of all samples on I_p-U_p curves

In this section the effect of the material of insulating tube on the I_p-U_p are shown in figures 5.29-5.30. It is evident that the material has no significant effect on the Ip-Up characteristics for both polarities of applied voltage.

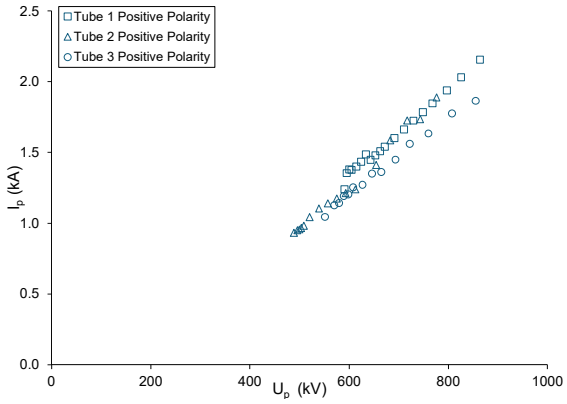

Figure 5. 29: I_p-U_p curves for IT 1,2 and 3 (+)

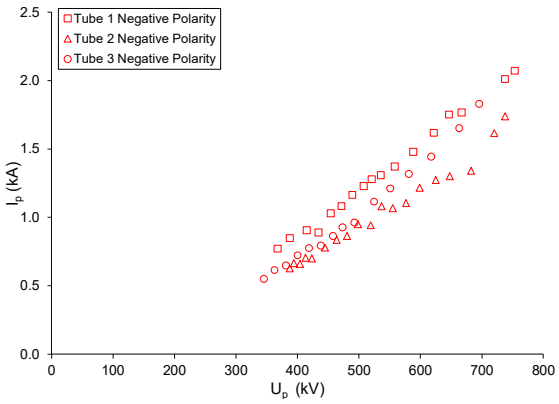

Figure 5. 30: I_p-U_p curves for IT 1,2 and 3 (-)

5.3 Flashover voltage- time to flashover characteristics (U_p-t_f)

In this section, the flashover voltage-time characteristics are presented for every insulating tube under positive and negative polarity of applied voltage in figures 5.31-5.36.

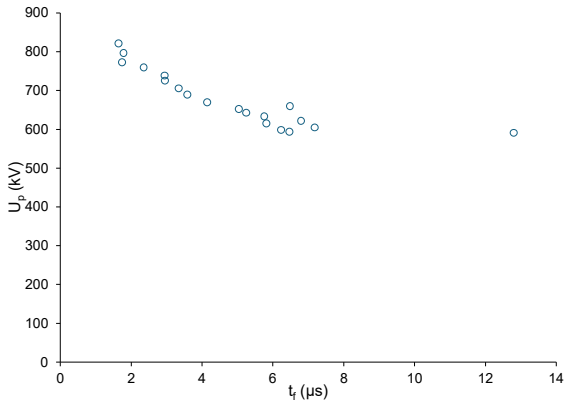

Figure 5.31: U_p-t_f curve for IT 1

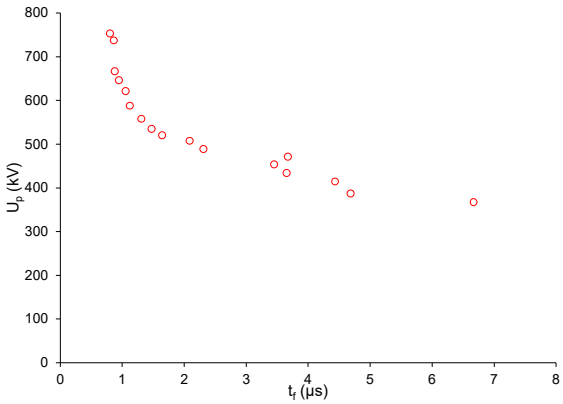

Figure 5.32: U_p-t_f curve for IT 1 (-)

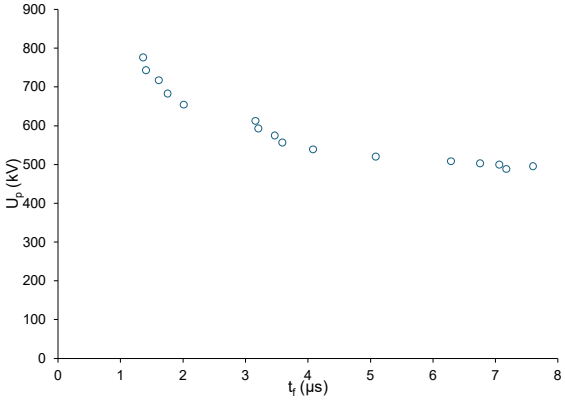

Figure 5.33: U_p-t_f curve for IT 2 (+)

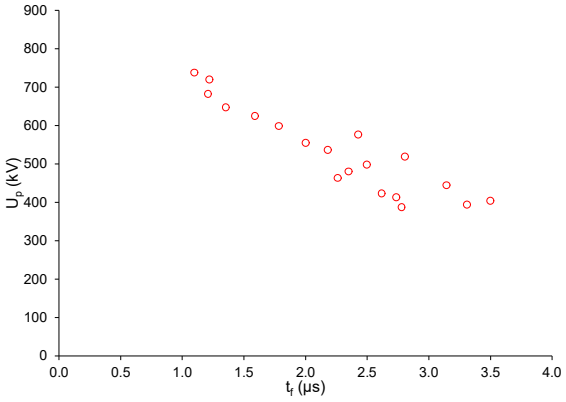

Figure 5.34: U_p-t_f curve for IT 2 (-)

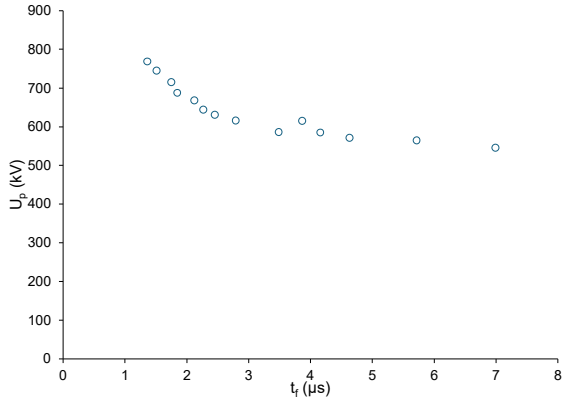

Figure 5.35: U_p-t_f curve for IT 3 (+)

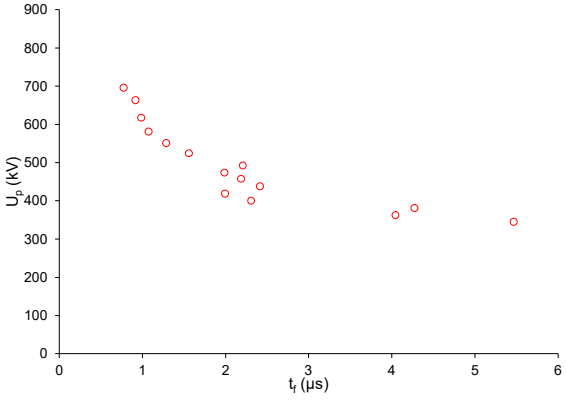

Figure 5.36: U_p-t_f curve for IT 3 (-)

From diagrams 5.31-5.36, it is observed that the increasing applied voltage, flashover

voltage increases while the time to flashover decreases, reaching a minimum value for the highest applied voltage levels. At higher levels the flashover voltage increases but the flashover time stabilizes. At lower levels of applied voltage, large dispersion of the time to flashover was observed, leading to higher time lags.

5.3.1 Effect of polarity on U_p-t_f curve

In this section, the characteristics U_p-t_f curves are presented for each insulating tube with the effect of polarity as affecting parameter in figures 5.37-5.39.

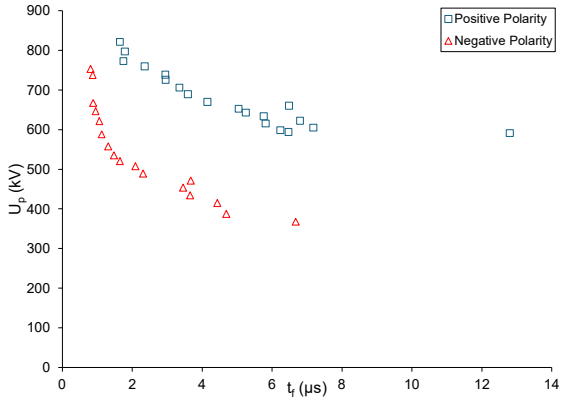

Figure 5.37: U_p-t_f curve for IT 1

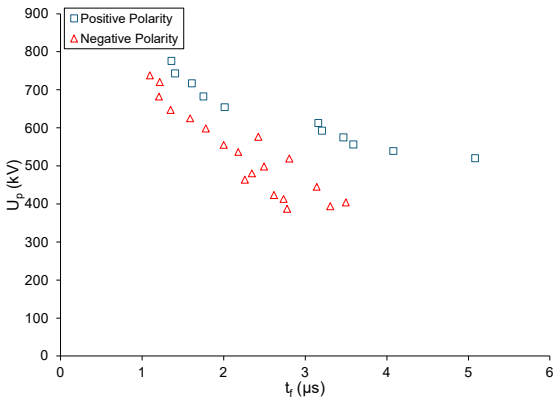

Figure 5.38: U_p-t_f curve for IT 2

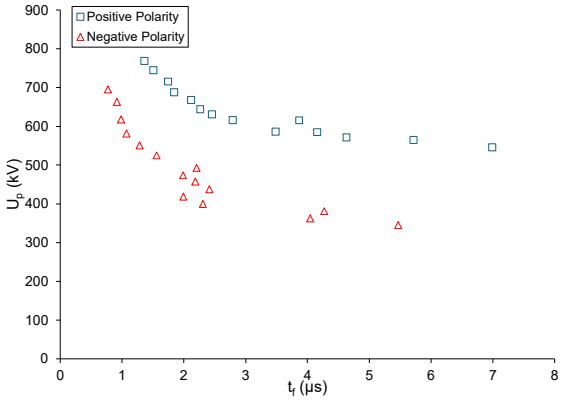

Figure 5.39: U_p-t_f curve for IT 3

It is evident that for the same time to flashover, the flashover voltage is higher under positive than negative polarity impulses, indicating better withstand capability compared to negative impulses. For higher voltages and shorter decay times, the effect of polarity on the U-t characteristics is less pronounced, as the curves tend to coincide. The negative

polarity curve appears to have a steeper slop implying that the flashover voltage changes more rapidly with respect to flashover time compared to positive polarity.

5.3.2 Effect of material on U_p-t_f curve

In this section, in figures 5.40-5.41, the effect of material of the insulating tubes on U_p-t_f is examined.

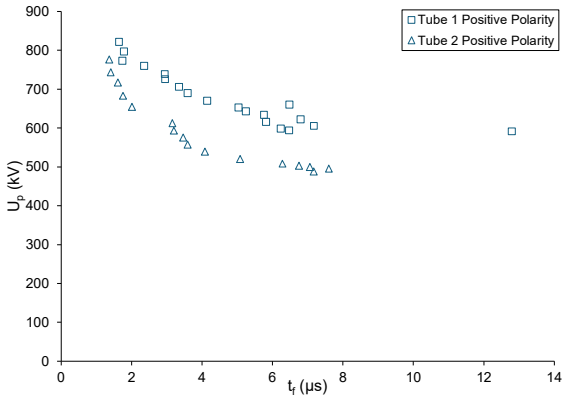

Figure 5.40: U_p-t_f curve for IT 1 and 2 (+)

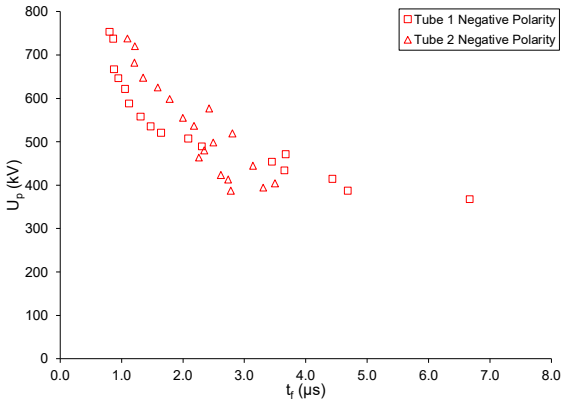

Figure 5.41: U_p-t_f curve for IT 1 and 2 (-)

The curve for tube 2 is lower as compared to the tube 1 which means tube 2 breaks down at lower voltages or shorter times compared to tube 1 under positive polarity. Tube 2 material is less resistant to positive polarity stress, likely due to poorer electron emission suppression or lower dielectric strength.

In case of negative polarity, curve for tube 1 is lower as compared to tube 2 which means that tube 1 breaks down at lower voltages or shorter times compared to tube 2 under negative polarity. So, tube 1 material is more susceptible to negative polarity stress, likely due to higher ion mobility or surface charging effects.

5.3.3 Effect of geometry on U_p-t_f curve

In this section, in figures 5.42-5.43, the effect of geometry of the insulating tubes on U_p-t_f is examined.

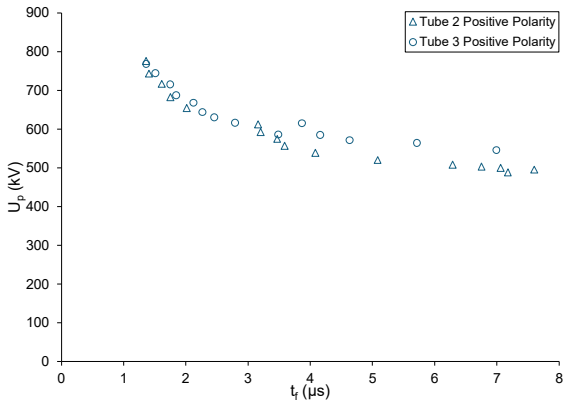

Figure 5.42: U_p-t_f curve for IT 2 and 3 (+)

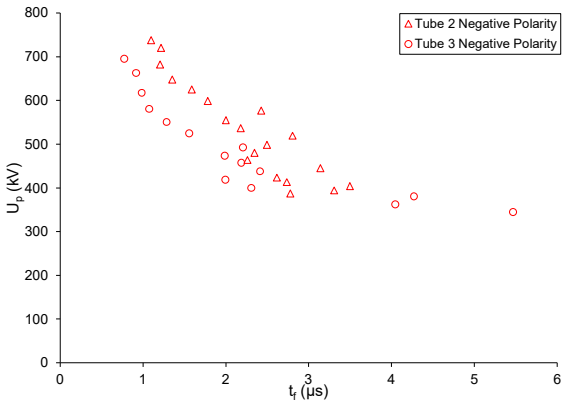

Figure 5.43: U_p-t_f curve for IT 2 and 3 (-)

Tube 3 has an extra insulating layer on the top and bottom while tube 2 does not have. This additional layer introduces interfaces between the materials which can be trap charges, create localized regions of high electric strength and acts as initiation points for flashover. Tube 2 has no additional layer, so its surface is more uniform and freer from interfaces or defects. This uniformity makes it harder for flashover to initiate, resulting in higher flashover voltage-time characteristics.

5.3.4 Effect of all samples on U_p-t_f curve

In this section, in figures 5.44-5.45, the effect of material and geometry of the insulating tubes on U_p-t_f is examined.

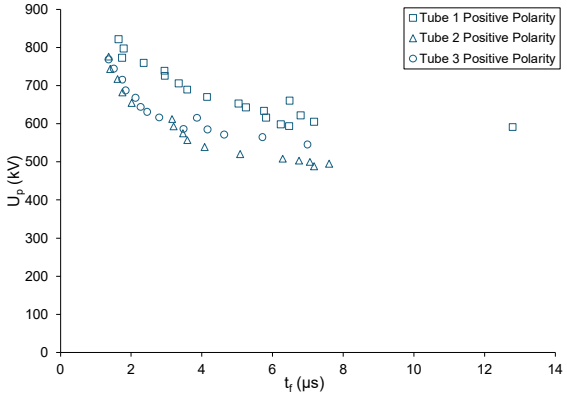

Figure 5.44: U_p-t_f curve for IT 1,2 and 3 (+)

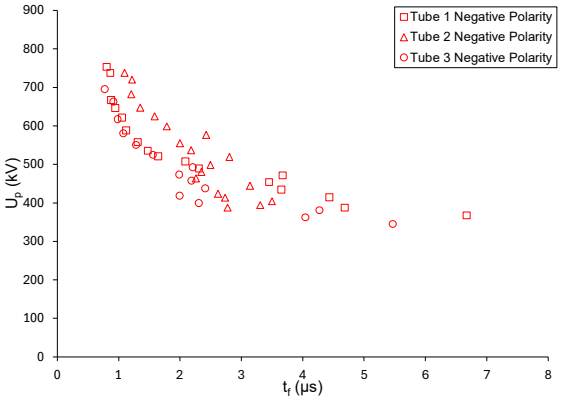

Figure 5.45: U_p-t_f curve for IT 1,2 and 3 (-)

The curves seem to exhibit some curvature, particularly at shorter flashover times. This

suggests a non-linear relationship between flashover voltage and flashover time.

5.4 Spark conductance as a function of the applied (I_p/U_p-U_{ap})

The purpose of extracting I_p/U_p-U_{ap} curves is to study the conductance of the spark channel at flashover. Figures 5.46-5.51 show the spark conductance curves for each insulating tubes and polarity of applied voltage.

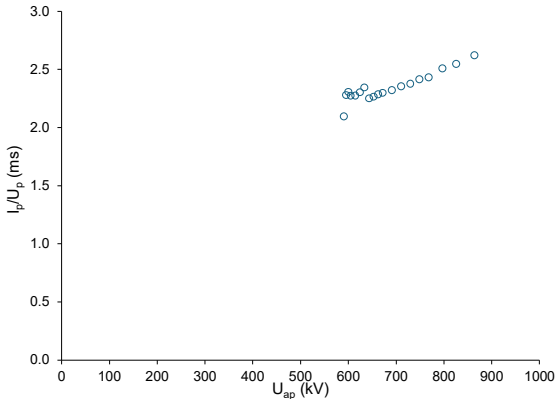

Figure 5.46: I_p/U_p, U_{ap} curve for IT 1 (+)

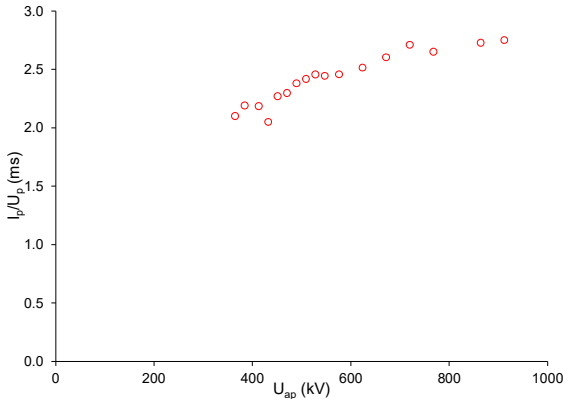

Figure 5.47: I_p/U_p, U_{ap} curve for IT 1 (-)

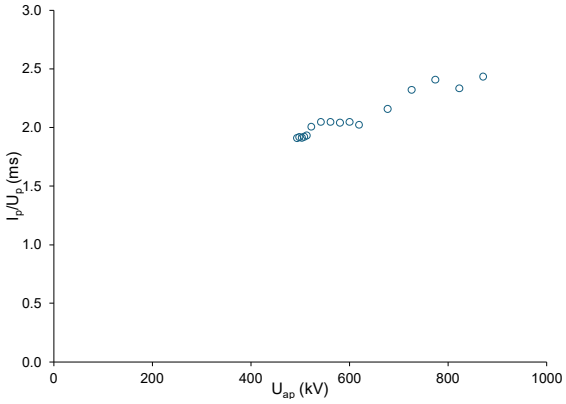

Figure 5.48: I_p/U_p, U_{ap} curve for IT 2 (+)

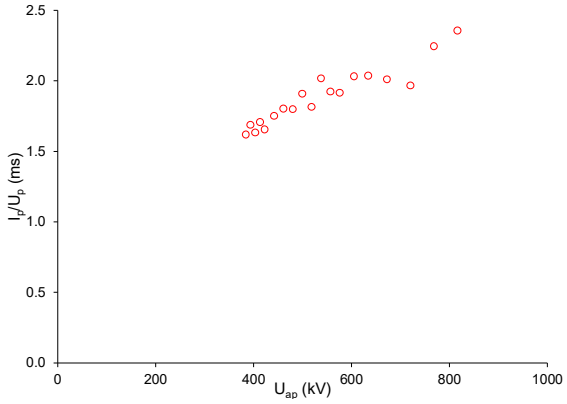

Figure 5.49: I_p/U_p, U_{ap} curve for IT 2 (-)

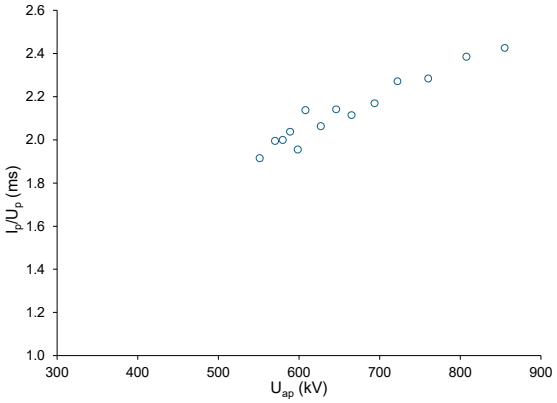

Figure 5.50: I_p/U_p, U_{ap} curve for IT 3 (+)

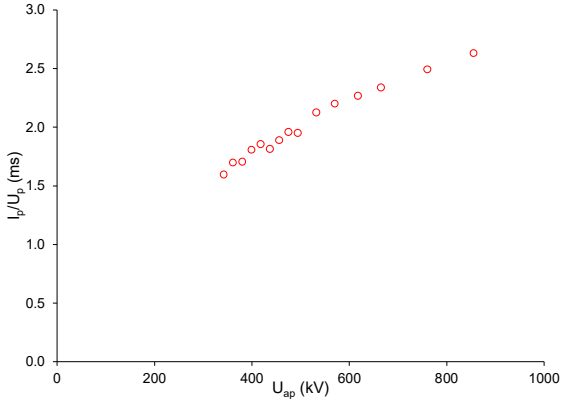

Figure 5.51: I_p/U_p, U_{ap} curve for IT 3 (-)

It is observed that spark conductivity remains nearly constant at relatively low applied voltages. After a threshold voltage value, the spark conductivity increases.

5.4.1 Effect of polarity on I_p/U_p-U_{ap} curve

In this section, the curves I_p/U_p-U_{ap} curves are presented for each insulating tubes to investigate the effect of polarity shown in figures 5.52-5.54.

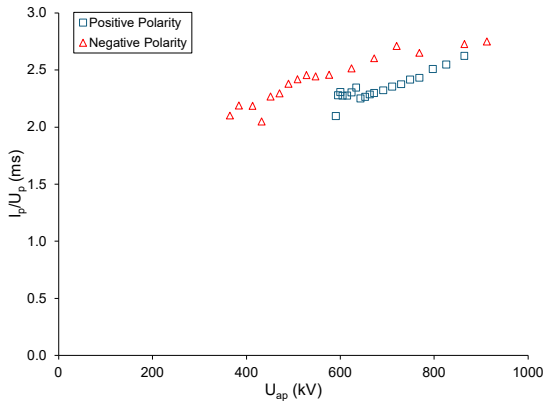

Figure 5.52: I_p/U_p, U_{ap} curve for IT 1

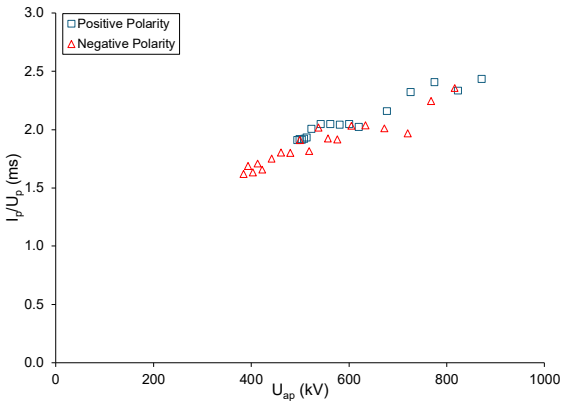

Figure 5.53: I_p/U_p, U_{ap} curve for IT 2

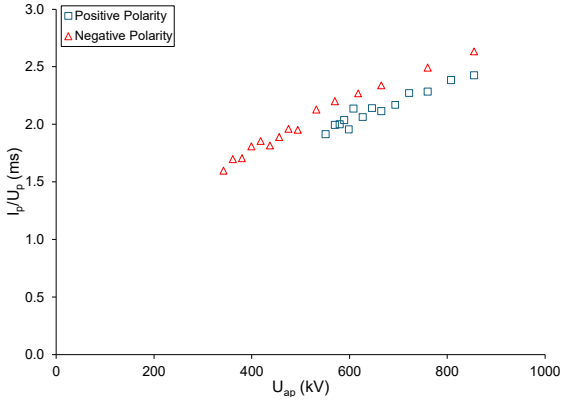

Figure 5.54: I_p/U_p, U_{ap} curve for IT 3

Under negative polarity, the conductance of the spark channel is generally higher except for figure 5.52. It was observed that under negative polarity, the discharge tends to develop on the surface of the insulating tube, while on the positive polarity it is mainly developed through air, away from the surface. With this together in fact that higher levels of conductance of the spark channel are observed under negative polarity impulses, it indicates that the surface of the insulating tubes enhances the development of the discharge resulting in higher spark channel conductivity.

5.4.2 Effect of material on I_p/U_p-U_{ap} curve

In this section, in figure 5.55-5.56, the effect of material on I_p/U_p-U_{ap} curves is examined.

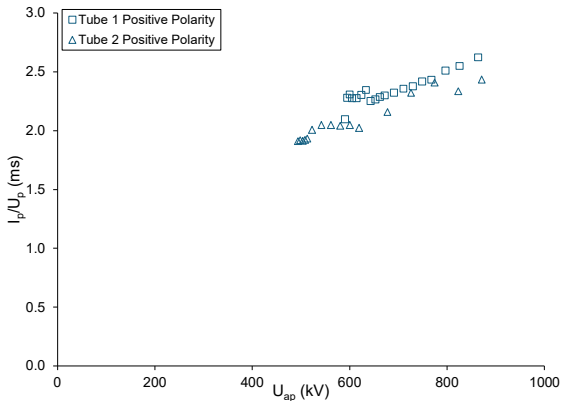

Figure 5.55: I_p/U_p, U_{ap} curves for IT 1 and 2 (+)

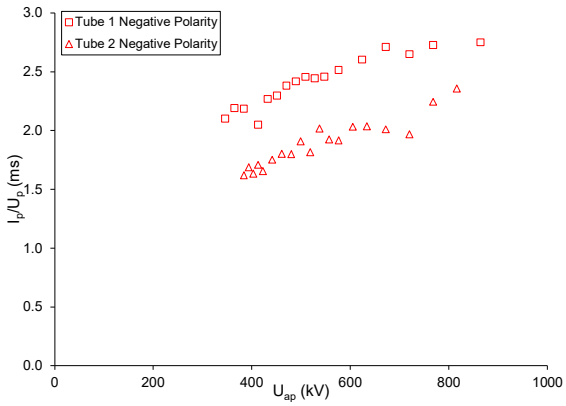

Figure 5. 56: I_p/U_p, U_{ap} curves for IT 1 and 2 (-)

The above graph illustrates that the conductivity of the tube 1 and tube 2 for positive polarity is similar. But in case of negative polarity, the conductivity of tube 1 is greater than that of the tube 2. This means that tube 1 could have a material that facilitates better electron flow or ion mobility under negative polarity whereas tube 2 might have a material that hinders electron flow or ion mobility under negative polarity, leading to lower conductivity. Under negative polarity, Tube 1 might experience less polarization (e.g., formation of insulating layers or charge buildup) compared to Tube 2. This would result in higher conductivity in Tube 1.

In case of positive charge, both tube 1 and tube 2 facilitate similar charge transport mechanisms. The similarity in conductivity under positive polarity suggests that the system is symmetric or balanced in this configuration. However, under negative polarity, inherent asymmetries in material properties, electrode behavior, ion mobility, or structural differences become more pronounced, leading to the observed difference in conductivity between Tube 1 and Tube 2.

5.4.3 Effect of geometry on I_p/U_p-U_{ap} curve

In this section, in figure 5.57-5.58, the effect of dimension on I_p/U_p-U_{ap} curves is examined.

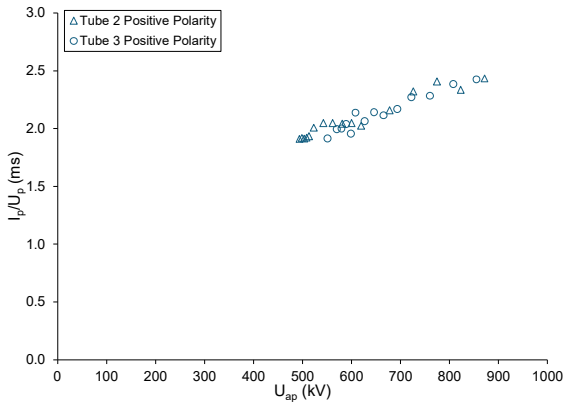

Figure 5.57: I_p/U_p, U_{ap} curves for IT 2 and 3 (+)

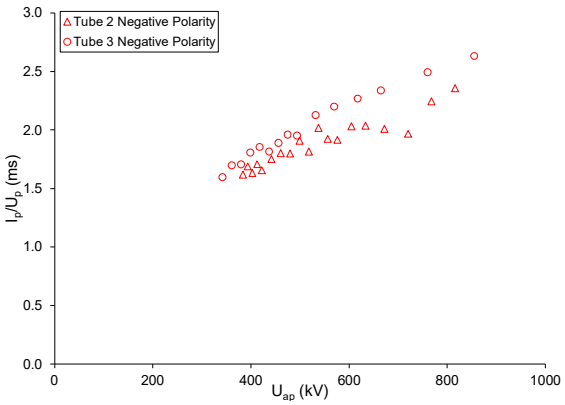

Figure 5.58: I_p/U_p, U_{ap} curves for IT 2 and 3 (-)

Under positive polarity, the electric field distribution is more uniform, and the additional insulating layer in tube 3 does not significantly alter the overall behavior. The conductivity is dominated by the bulk properties of the insulating material which are the same for both tubes. The additional layer in tube 3 does not introduce significant defects or non-uniformities that would affect the conductivity under positive polarity Under negative polarity, the additional layer in tube 3 introduces effects that enhance the local electric field and provide sites for secondary electron emission. These effects lead to greater conductivity in tube 3 compared to tube 2.

5.4.4 Effect of all samples on I_p/U_p-U_{ap} curve

In this section, in diagram 5.59-5.60, the effect of material and geometry on I_p/U_p-U_{ap} curves is examined.

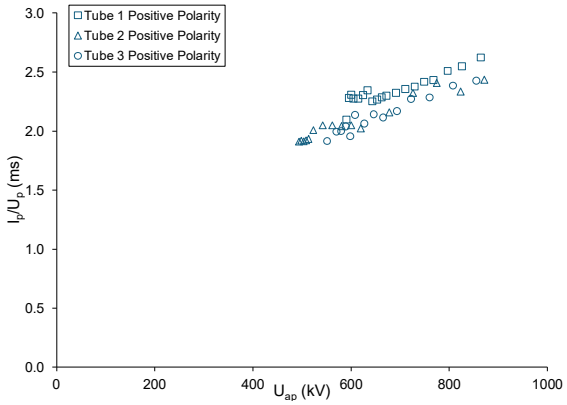

Figure 5.59: I_p/U_p, U_{ap} curves for IT 1,2 and 3 (+)

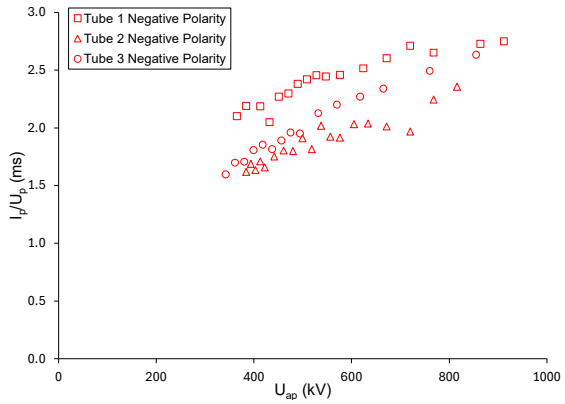

Figure 5.60: I_p/U_p, U_{app} curves for IT 1,2 and 3 (-)

A general upward trend is observed indicating that as the applied voltage (U_{ap}) increases, the ratio of current to voltage (I_p/U_p), which represents conductance, also increases. This is expected, as higher voltage leads to greater ionization and charge movement within the insulating material, facilitating spark formation and conduction.

So, for all the scenarios, we can see that the negative polarity is more severe than the positive polarity which can be described in terms of plasma physics. The breakdown of an insulating tube under high voltage is governed by plasma formation mechanisms that differ notably between positive and negative polarities. Key processes such as electron avalanches, streamer propagation, space charge effects, and electrode interactions play a role. Negative polarity typically results in more pronounced breakdown, driven by enhanced electron emission, stronger field distortion, and localized plasma instabilities. When an insulating tube undergoes streamer-dominated breakdown, the process starts with electron avalanches triggered by free electrons near the anode. These electrons accelerate in the electric field, colliding with and ionizing gas molecules, which forms a conducting plasma path. The slower-moving positive ions left behind intensify the local electric field near the tube's surface, encouraging secondary electron emission and further sustaining the discharge.

The streamer advances primarily through photoionization: ultraviolet (UV) photons emitted by the excited plasma ionize nearby gas molecules, allowing the discharge to propagate. Unlike a full spark or arc, this breakdown remains partially controlled because the buildup of space charge (excess ions and electrons) weakens the local electric field, preventing runaway ionization. Depending on factors like gas pressure and how quickly the voltage rises, the resulting plasma may appear as either thin, branching filaments or a more diffuse, spread-out streamer.

Electrical breakdown under negative polarity conditions is significantly more intense than under positive polarity due to fundamental differences in discharge physics. The process begins at the cathode, where electrons are liberated through both field emission and secondary emission caused by ion bombardment. These electrons form dense avalanche clusters in the high-field region near the cathode surface. While the negative potential rapidly accelerates electrons away from the cathode, the slower positive ions accumulate,

creating a concentrated space charge layer that dramatically enhances and distorts the local electric field. This leads to the formation of aggressive cathode-directed streamers and, in high-current situations, the development of destructive cathode spots - microscopic plasma zones with extreme current densities that cause rapid electrode erosion through thermal and sputtering effects. The resulting discharge exhibits distinct characteristics including highly filamentary plasma channels, substantially elevated current densities, intense localized gas heating, and significant molecular dissociation of the insulating medium. These effects are further amplified by the pronounced space charge accumulation near the cathode, which creates additional field enhancement and accelerates the breakdown process compared to positive polarity conditions.

Thus, the negative polarity is more severe as:

i. Negative polarity facilitates stronger secondary electron emission from the cathode, sustaining a denser plasma.

ii. Positive ions near the cathode enhance local fields, leading to runaway ionization.

iii. Localized plasma spots increase material erosion and gas decomposition, accelerating ionization.

iv. Cathode-initiated streamers are more filamentary and conductive, leading to rapid plasma channel formation.

CHAPTER SIX: CONCLUSION

A Lightning Protection System (LPS) is a system designed to protect electrical infrastructure from lightning strikes by safely directing high-voltage surges to the ground. It consists of air terminals, down conductors, and grounding systems that dissipate lightning energy. By preventing damage to transmission and distribution systems, LPS reduces outages and equipment failures. It minimizes power disruptions, ensuring stable and continuous electricity supply. Overall, an effective LPS enhances system reliability by protecting critical components from lightning-induced faults.

Experiments were conducted to investigate the flashover characteristics of insulating tubes on differing in geometry and material under positive and negative lightning impulses. The lightning impulse was produced using a Marx generator and applied to the air termination. The devices were grounded through a suitable cable that passes through the voltage transformer for current measurement purposes and end at the grounded floor. The output of the current transformer ended up via a suitably shielded cable to the signal attenuator which was connected to the oscilloscope. With all this equipment, the flashover characteristics of the insulating tubes under positive and negative lightning impulse have been investigated. The number of shots is applied on each voltage level and using the multi-level method, the probability of the flashover is measured. The discharge current, voltage and the gap conductance at flashover were measured and analyzed. Different curves were plotted with which the flashover characteristics have been discussed.

The experimental results and by extension the diagrams that were extracted and concerned the dielectric behavior of the insulators, were examined under the influence of the waveform and the polarity of the imposed voltage. For all the insulating tubes, the U_{50} for negative polarity is always lower than that of positive polarity which means the tube possesses higher dielectric strength for positive polarity than the negative polarity.

It has been observed that the discharge current is higher under negative than the positive polarity impulses, with the effect being similar for all the insulating tubes. Generally, with increasing applied voltage the discharge current increases linearly with flashover voltage. The maximum discharge current-applied voltage curves (I_p-U_{ap}) have shown that the polarity effect is rather minimal.

The flashover time for positive polarity is higher compared to negative polarity for the same applied voltage. For higher voltages and shorter flashover times, the effect of polarity on the U-t characteristics is less pronounced, as the curves tend to coincide. The negative polarity curve appears to have a steeper slop implying that the flashover voltage changes more rapidly with respect to flashover time compared to positive polarity. Under negative polarity, the conductance of the spark channel is generally higher than positive as negative polarity facilitates the spark from the surface whereas the positive polarity away from the surface i.e. from air. The spark conductance is constant up to certain voltage level. After a threshold voltage level, spark conductivity increases.

For positive polarity, tube 1 has the highest dielectric strength but has the least for negative polarity. Tube 1 shows a different behavior with the conductivity on both gap and material during positive polarity. Generally, conductivity is higher, indicates high spark conductance and lower dielectric strength. But in the case of tube 1, it has higher spark conductance as well as higher dielectric strength. At higher levels of applied voltage two or more sparks were observed in some cases. Sparks with a common starting point or even coalescing of two different sparks before fully crossing the gap have also been observed. The existence of two sparks can also be distinguished from the waveforms of the resulting currents which present in several cases double peaks and other types of fluctuations that need further study. So, the flashover mechanism is dependent on the material and the geometry of the tube used.

CHAPTER 7: SUGGESTION FOR FURTHER RESEARCH

At this point it can now be stated that the conclusions reached in the context of this laboratory thesis are of key importance, however the subject needs further research. In addition, the experimental examination of the effect of pollution and humidity, as well as atmospheric conditions, is also important.

More information can be extracted from the already existing data. From the data not used in this thesis and mainly from the correlation of voltage, current as well as flashover time, useful conclusions can be drawn about the electrical flashover mechanism of insulating tube, thus helping to better understanding of the physical mechanisms underlying the electrical flashover phenomenon. Furthermore, the importance of the effect of the spark path on the flashover times and the discharge current range needs further investigation which can be carried out by using a camera during the experimental procedure. The impact of temperature, humidity, and atmospheric pressure on flashover probability and dissociation time should be examined. These parameters could significantly affect the reliability of the tubes in real-world applications. To improve the reliability of findings, future research could involve testing a larger sample size and performing advanced statistical analysis. Monte Carlo simulations or machine learning models could be applied to predict flashover behavior under various conditions.

Based on the flashover probability curves, future studies could investigate protective coatings, insulation techniques, or material modifications to improve flashover withstand. Research into field-grading methods or surface treatments could offer practical solutions for enhancing tube performance under high-voltage conditions. To assess long-term reliability, future studies should evaluate how repeated lightning discharges and prolonged electrical stress affect material degradation, mechanical integrity, and electrical properties over time. This would be essential for applications requiring high durability and longevity.

Similarly, the investigation with other impulse waveform than the 1.2/50 μs such as the 0.34/47 μs should be done as because different lightning waveforms represent different stress conditions on materials and structures. The 0.34/47 μs waveform has a faster rise time (0.34 μs), meaning it applies a sharper, more intense voltage stress. This simulates restrikes or induced surges, which may cause different failure mechanisms. So further

proper research is needed to ensure the behavior of different insulating tubes under different conditions for reliable and effective lightning protection systems.

REFERENCES

[1] P. N. Mikropoulos, "Laboratory Exercises in High Voltage Technology", High Voltage Notes I and II, Thessaloniki, 2008

[2] IEC 60060-1: "High-voltage test techniques, Part1: General definitions and requirements", 2010.

[3] Mitchell Guthrie, Greg Martinjak, Harold Bud VanSickle, "IEC 62561 electrical testing of US connectors and stranded cable", *2016 33rd International Conference on Lightning Protection (ICLP)*, pp.1-9, 2016.

[4] S. Faufeaix, "Investigation and studies on Lightning Air Terminal shape in relationship with the efficiency of a simple rod ", the International Lightning Protection Association Symposium, 2014.

[5] Richard Chadwick, "The Comparison of Lightning Protection System (LPS) in Accordance with NFPA 780 and IEC 62305-3", 2016

[6]. EC 62305-3, Protection against lightning – Part 3: Physical damage to structures and life hazard, 2010.

[7] I.B. Cohen (Ed.), Experiments and Observations on Electricity, Harvard University Press, Cambridge (1962)

[8] Mitchell Guthrie, Greg Martinjak, Harold Bud VanSickle, "IEC 62561 electrical testing of US connectors and stranded cable", *2016 33rd International Conference on Lightning Protection (ICLP)*, pp.1-9, 2016.

[9] Zhang, L., et al. "Study on the Performance of Lightning Protection Systems with Insulated Air Terminals." *Journal of Lightning Protection Technology*, 2021.

[10] Liu, X., & Zhang, Y. (2021). Application of insulated air terminals in modern lightning protection systems. Journal of Electrical Engineering and Technology, 46(1), 123-130.

[11] Protected Volume of Lightning Air-Termination Systems. (2022). doi: 10.1109/icps54075.2022.9773942

[12] W. Hauschild and E. Lemke, *High-Voltage Test and Measuring Techniques*. Springer, 2010.

[13] E. Kuffel, W.S. Zaengl, and J. Kuffel, *High Voltage Engineering: Fundamentals*, 2nd ed. New York, NY: McGraw-Hill, 2000.

[14] He, Zhenghao., Xu, Huaili., Bai, Jing., Yu, Fusheng., Hu, Feng., Li, Jin. A Test Study of 50% Lightning Impulse Breakdown Voltage on Rod-Plane Gap with Two-Phase Mixture of Gas and Solid Particles. Plasma Science & Technology, (2007).;9(6):695-697. doi: 10.1088/1009-0630/9/6/12

[15] Indhika, Fauzhan, Warsito., Muhammad, Faudzi, M, Yasir., Muhammad, Akmal, Abu, Taib., Eko, Supriyanto., Indhina, Reihannisha., N., F., Kasri. Double Air Terminal in Lightning Protection System. (2019). doi: 10.1109/IEEECONF48524.2019.9102533

[16] Dev. (2022, March 22). An overview of the key elements of a lightning protection system. Kingsmill Industries. https://kingsmillindustries.com/key-elements-of-lightning-protection-system/

[17] J. A. Martinez-Velasco, J. Arturo, and Samir Bedoui, "Lightning Performance Analysis of Transmission Lines Using Parallel Computing," *ResearchGate*, Sep. 12, 2016. https://www.researchgate.net/publication/308335329_Lightning_Performance_Analysis_of_Transmission_Lines_Using_Parallel_Computing (accessed Apr. 18, 2025).

APPENDIX A: PUBLICATION

Gmail

Akrit Acharya <erakritacharya@gmail.com>

[IOEGC16] Editor Decision

1 message

Suwarna Lingden <conference-noreply@ioe.edu.np> Wed, Apr 2, 2025 at 8:37 AM
To: AKRIT ACHARYA <erakritacharya@gmail.com>, Basanta Kumar Gautam <basanta.gautam@pcampus.edu.np>

AKRIT ACHARYA, Basanta Kumar Gautam:

We are pleased to inform you that your manuscript titled "Experimental investigation of the surface dielectric strength of insulating tubes supporting air terminals of electrically insulated lightning protection systems under standard lightning impulse voltages" submitted to 16th IOE Graduate Conference is **Accepted** for presentation in the Conference as well as inclusion in the Peer-Reviewed Proceedings. Please note that inclusion in hard copy proceedings is contingent upon your timely response to further edits, if any, during the publication process.

With Warm Regards,
IOEGC-16 Editorial Team

IOE Graduate Conference
[Placeholder for Publication Information]

Experimental investigation of the surface dielectric strength of insulating tubes supporting air terminals of electrically insulated lightning protection systems under standard lightning impulse voltages

Akrit Acharya[a], Basanta Kumar Gautam [b]

[a,b] *Department of Electrical Engineering, Pulchowk Campus, Institute of Engineering, Tribhuvan University, Nepal*
[a] 079mspse001.akrit@pcampus.edu.np

Abstract
Lightning Protection Systems (LPS) safeguard structures, electrical systems, and personnel from lightning strikes. A critical component, insulating tubes, provides electrical isolation and directs current properly. These tubes must withstand extreme lightning-induced shocks, often reaching hundreds of kilovolts, while retaining insulating properties. Evaluating their performance under standardized lightning impulse voltages (1.2/50 µs) is essential due to their transient, high-voltage nature. Key factors influencing performance include voltage polarity, material composition, tube geometry, and environmental conditions. Unlike steady voltage tests, lightning impulse conditions reveal distinct behaviors, necessitating specialized assessments to ensure reliability. Failure of these tubes can compromise the entire LPS, highlighting the need for rigorous testing. This study investigates the dielectric properties of insulating tubes under both positive and negative lightning impulses, analyzing their response to rapid voltage escalation. By assessing surface dielectric strength, the research enhances understanding of system reliability in real-world lightning scenarios, aiding in the selection and optimization of insulating materials for robust lightning protection.

Keywords
Lightning Protection system, insulating tubes, air termination, Marx Generator

1. Introduction

Lightning Protection Systems (LPS) are regularly incorporated in the construction of buildings and structures that are susceptible to lightning strikes. In case the current from a lightning stroke can inflict damage to the object being protected or its conductive elements or cause damageable sparking, then LPS lightning protection systems that are electrically insulated are used [1]. So, knowledge on the lightning impulse behavior of the latter has been of great interest since the pioneering works done since the 1950s [2-5]. According to IEC 60060-1:2010 [6], an impulse is a periodic voltage or current pulse period whose action is level controlled and whose maximum level is reached and returned to zero at a significantly slower pace.

Components such as clamps and conductors, conductors, air termination rods, earth electrodes, conductor fasteners, isolating spark gaps, and soil improvement chemicals are covered under the seven sections of IEC 62561 [7]. The flashover voltage of critical impulse, or CFO, which is the crest value of the typical flashover voltage that causes 50% flashover probability, is frequently used to measure the flashover performance of flashover equipment for insulation coordination in analytical investigations [8].

The purpose of a lightning protection system's (LPS) air termination system is to safely divert lightning discharge currents to the earth. In order to effectively protect structures, it consists of conductor grids, aerial rods, and catenary conductors [9]. A nonconductive insulating tube encircles a conductive metal rod or terminal (such as copper or aluminum) in an air terminal with an insulating tube. This insulating layer prevents side flashover, improves durability, protects against corrosion, and isolates electrical current.

The study of an insulating tube is a critical component of an isolated lightning protection system. Insulating

tube is a component of air termination system. It is a hollow structure with an insulating material on the surface.

Figure 1: Insulating tube in real application

Figure 1 presents the general layout of the insulation tube. Once the lightning strikes the air termination, the insulating tube restricts the flow of voltage and provides the intended flow through a down conductor. Insufficient research has been done on the surface dielectric strength of electrically insulating tubes that support air terminals in lightning protection systems under conditions that simulate lightning impulses. This could result in insufficient lightning protection and system failures. For electrical systems to remain safe and reliable during lightning strikes, the flashover mechanism in lightning protection air terminations is essential. This process entails the disintegration of the air insulation, which causes the electricity to discharge quickly. Designing efficient lightning protection systems requires an understanding of the variables affecting flashover behavior.

The insulating tube supporting air terminations at standard lightning impulse voltages (1.2/50 μs) of positive and negative polarity is experimentally investigated in depth in this paper. Impact high voltages are classified as internal (SI) or external (LI) based on the length of time their front lasts. This paper discusses the impact of the applied voltage's polarity on the breakdown mechanism.

2. Experimental arrangement and measurement procedure

The experimental measurements were carried out in the High Voltage laboratory of the Aristotle University of Thessaloniki. Standard lightning impulse voltages of both polarities were applied to the air termination system with an insulating tube of height 1 m using a 10-stage Marx generator 1MV/7kJ (Figure 2). The applied impulse voltage and the discharge current were recorded (Figure 3) using capacitive divider of the Marx generator and a Pearson 301X current transformer, respectively, together with a LeCroy WR64Xi oscilloscope.

Flashover probability distributions were obtained by applying the multi-level method according to IEC 60060-1 Standard [6]. The probability distribution was evaluated collecting data for withstand and flashover, plotting breakdown data and using statistical fitting method. Mean breakdown voltage, variance and then the standard deviation was evaluated.

To study the effects of the impulse voltage peak on discharge characteristics the air termination was overstressed; at least 10 impulse shots at voltage levels higher than causing 100% flashover probability where applied. Salient characteristics of the discharge flashover, namely voltage, time and current were measured.

Figure 2: Experimental setup

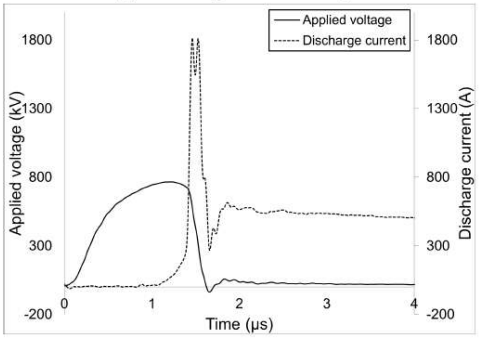

Figure 3: Applied voltage and discharge current oscillographic records (positive polarity)

Experiments were performed at ambient atmospheric conditions (T = 17°C, P = 768 mmHg, h = 11.96 gm^{-3})

3. Experimental results and discussions

The imposed open circuit voltage for positive and negative polarity is demonstrated in Figure 4 (positive polarity) and Figure 5 (negative polarity).

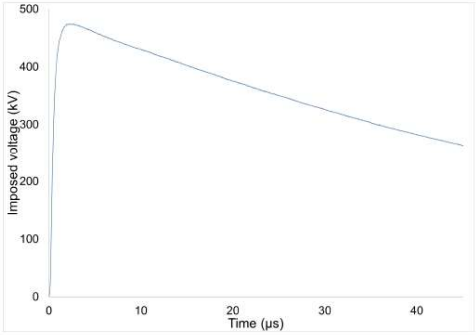

Figure 4: 50 kV positive polarity imposed waveform

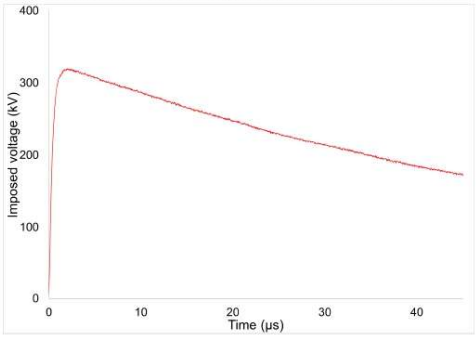

Figure 5: 34 kV negative polarity imposed waveform

3.1 Breakdown probability curve

Figure 6 shows the breakdown probability distributions of the investigated insulating tubes as obtained through the multiple level test method.[**?**] The distributions were well approximated by the normal distribution; thus, the 50% breakdown voltage, U_{50}, and standard deviation, σ, were calculated.
Positive polarity is shown to have a breakdown probability curve that is to the right of the equivalent one, meaning that U_{50} is higher for positive polarity. For positive polarity, a larger U_{50} means that the material or system can tolerate a higher positive voltage before breaking down than it can handle a negative voltage.

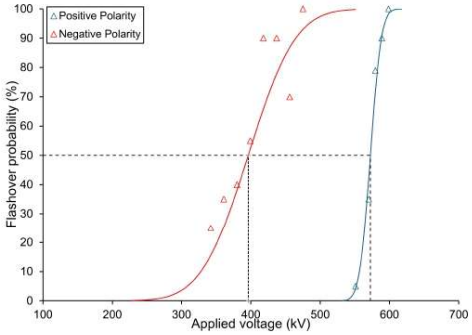

Figure 6: Breakdown probability curve

Table 1: U_{50} and σ for positive and negative polarity

Polarity	U_{50} (%)	σ (%)
Positive	572.38	2.16
Negative	396.15	13.5

A weaker electric field and a more gradual accumulation of charge are typical characteristics of positive lightning strikes close to the air termination system. This delayed development results in a greater U_{50} because it provides the insulating tube more time to resist disintegration. Rapid increases in electric field strength and the creation of electron avalanche are common features of negative lightning. For negative polarity, the U_{50} is decreased by this quick ionization. The standard deviation of negative polarity is greater than that of positive polarity in a breakdown probability curve indicating that the breakdown events for negative polarity are more variable and less predictable. This suggests that negative polarity might lead to more inconsistent breakdown behavior.

3.2 Maximum breakdown current-voltage curves, I_p-U_p

The I_p-U_p curves were constructed to enable the study of the resulting current as a function of the maximum breakdown voltage.

Because electrons are far more mobile than ions and can be released from the cathode more easily by field emission and secondary electron emission, the I_p-U_p curve is larger for negative polarity. The strong local electric field close to the cathode with negative polarity promotes ionization, which speeds up avalanche generation and raises breakdown currents. Ionization is further intensified by increased electron density brought on by space charge effects. Conversely, at the anode, heavier and slower positive ions predominate for positive polarity, which lowers the ionization rate and produces a smaller I_p-U_p curve.

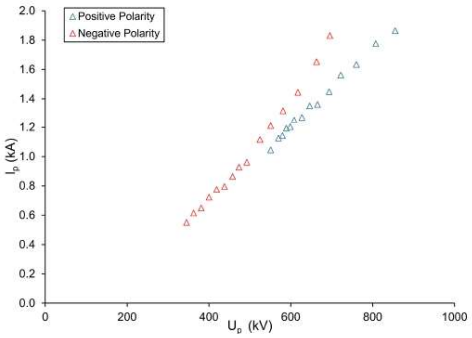

Figure 7: Maximum breakdown current-voltage curves

3.3 Maximum current-applied voltage curves, I_p-U_{app}

The maximum current-applied voltage curve in represents the electrical response of an insulating material or component when subjected to increasing voltage.

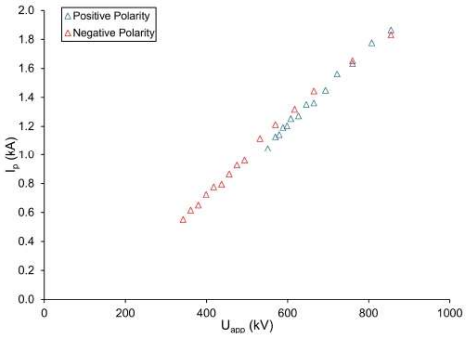

Figure 8: Maximum current-applied voltage curves

The I_p-U_{app} curve for both positive and negative polarity seems to be similar because the overall ionization and conduction mechanisms remain comparable. In high-voltage conditions, once the applied voltage exceeds the breakdown threshold, both polarities facilitate charge carrier generation and current flow through similar avalanche processes.. A

general conclusion drawn is the nearly linear relationship between peak current and applied voltage.

3.4 Dissociation voltage-dissociation time characteristic curves, U_p-t_f

The voltage-time curves are graphs which, for a series of voltage levels, depict the maximum value of each level as a function of the corresponding decay time. This voltage constitutes the maximum voltage applied to the gap, while the breakdown time was defined as the time at which the maximum value of the spark current appears.

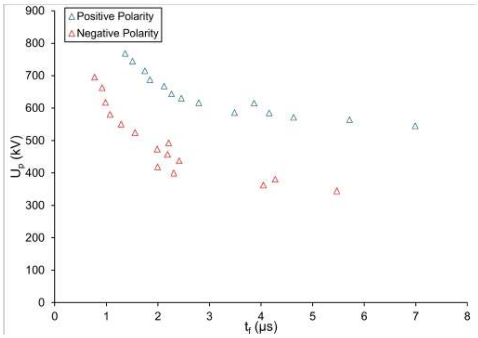

Figure 9: Dissociation voltage-dissociation time characteristic curvess

The U_t curves of positive polarity are always at a higher level than the corresponding ones for negative polarity, so for the same breakdown voltage, the breakdown time observed under positive polarity applied voltage is greater than the negative polarity. This indicates that insulating materials generally exhibit greater resistance to breakdown when subjected to positive polarity stresses compared to negative polarity stresses. The major effect of the polarity is observed in case of lower voltage level. For higher voltages and shorter decay times, the effect of polarity on the time-voltage (U_t) curves is noticeably smaller as the curves tend to coincide.

3.5 Spark conduction curves based on breakdown voltage per level, I_p/U_p, U_{app}

The I_p/U_p, U_{app} curves show the spark conductance based on the breakdown voltage per breakdown voltage level i.e. based on the maximum stress strains of the specimen. The purpose of their extraction is to study the conductivity presented by the material when it jumps over the material. A high I_p/U_p ratio suggests that the material allows more current to pass through for a given voltage, indicating higher conductivity during breakdown and vice versa.

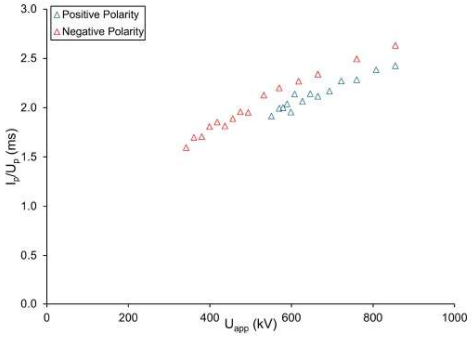

Figure 10: Spark conduction curves based on breakdown voltage per level

The ratio of $I_p/U_p$is greater in case of negative polarity than positive polarity which implies higher conductivity during the breakdown. Higher the conductivity, lower is the dielectric strength and U_{50} in general.

3.6 Spark conductance curves based on voltage at peak current per breakdown voltage level (I_p/U_p, I_p-U_{app})

The I_p/U_p, I_p-U_{app} curves shows the spark conductance based on voltage at maximum current.

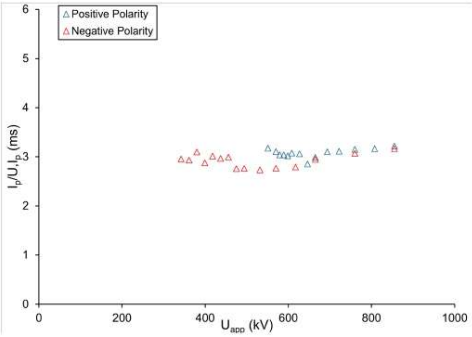

Figure 11: Spark conductance curves based on voltage at peak current per breakdown voltage level

The purpose of their extraction is the study of the

conductivity presented by the spark at the time of the breakdown. This conductivity differs from the conductivity value corresponding to the breakdown voltage as at the time of breakdown, the voltage is obviously lower than the breakdown voltage which is the maximum strain stress of the specimen.

The conductivity of the spark for both the positive and negative polarity is similar i.e. I_p/U_p, I_p-U_{app} is not affected much by polarity.

Conclusion

The breakdown characteristics of a insulating tube for both positive and negative polarity was presented in this paper. It was seen that the negative polarity has severe effect than positive polarity. Negative polarity intensifies the plasma effect in high voltage multi-level tests, when a plasma channel is formed around the test object as a result of enhanced air or gas ionization. This plasma generation speeds up breakdown by drastically reducing the material's dielectric strength. In contrast to positive polarity, the negative voltage attracts electrons, leading to greater ionization and a stronger plasma channel. Under negative polarity, breakdowns thus happen more quickly and frequently, which frequently results in lower U_{50} values and higher breakdown rates. One of the main causes of the observed variations in performance between polarities is the plasma effect. The effect of positive and negative standard lightning impulse voltage has been discussed. Further investigation is needed with the insulating tube having different geometry and materials. Similarly, the investigation with other waveform than 1.2/50 μs such as 0.34/4.7 μs should be done as because different lightning waveforms represent different stress conditions on materials and structures. The 0.34/4.7 μs waveform has a faster rise time (0.34 μs), meaning it applies a sharper, more intense voltage spike. This simulates restrikes or induced surges, which may cause different failure mechanisms.

Acknowledgement

This work was supported by the Department of Electrical Engineering and Computer Engineering Electricity Sector (High Voltage Laboratory) of Aristotle University of Thessaloniki Polytechnic School, Greece.

References

[1] IEC 62305-3, Protection against lightning – Part 3: Physical damage to structures and life hazard, 2010.

[2] J. H. Park and H. N. Cones, "Surge voltage breakdown of air in a nonuniform field," Journal of Research of the Natural Bureau of Standards, Vol. 56, No. 4, 1956.

[3] G. M. Petropoulos, "Constriction of a spark discharge during impulse breakdown," Br. J. Appl. Phys., Vol. 15, No. 2, pp. 169-176, 1964.

[4] R. T. Waters and R. E. Jones, "The impulse breakdown voltage and time-lag characteristics of long gaps in air I. The positive discharge," Philosophical Transactions of the Royal Society of London. Series A, Mathematical and Physical Sciences, vol. 256, no. 1069, pp. 213–234, 1964.

[5] E. Marode, "The mechanism of spark breakdown in air at atmospheric pressure between a positive point and a plane. I. experimental: Nature of the streamer track," J. Appl. Phys., vol. 46, no. 5, pp. 2005–2015, 1975.

[6] IEC 60060-1:2010, High Voltage Test Techniques-Part 1: General definitions and test requirements

[7] Mitchell Guthrie, Greg Martinjak, Harold Bud VanSickle, "IEC 62561 electrical testing of US connectors and stranded cable", 2016 33rd International Conference on Lightning Protection (ICLP), pp.1-9, 2016.

[8] IEEE Std. 1410-2010: Guide for improving the Lightning Performance of Electric Power Distribution Lines, Jan. 2011.

[9] Kurniawan, S., Purwanto, S., & Nursitao, E. D. (2024). Air Termination Of Lightning Protection For The Buildings Which Containing Solid Flammable Materials. Asian Journal of Engineering, Social and Health,3(2),381–329

APPENDIX B: PLAGIARISM TEST REPORT

Akrit Acharya

Experimental Investigation of the Surface Dielectric Strength of Insulating Tubes Supporting Air Ter

Tribhuvan University

Document Details

Submission ID
trn:oid:::3117:450686490

Submission Date
Apr 20, 2025, 3:25 PM GMT+5:45

Download Date
Apr 20, 2025, 3:27 PM GMT+5:45

File Name
Experimental Investigation of the Surface Dielectric Strength of Insulating Tubes Supporting Air ....pdf

File Size
4.1 MB

71 Pages

17,989 Words

90,286 Characters

iThenticate Page 1 of 77 - Cover Page Submission ID trn:oid:::3117:450686490

10% Overall Similarity

The combined total of all matches, including overlapping sources, for each database.

Match Groups

- **139** Not Cited or Quoted 10%
  Matches with neither in-text citation nor quotation marks
- **0** Missing Quotations 0%
  Matches that are still very similar to source material
- **0** Missing Citation 0%
  Matches that have quotation marks, but no in-text citation
- **0** Cited and Quoted 0%
  Matches with in-text citation present, but no quotation marks

Top Sources

- 7% Internet sources
- 7% Publications
- 0% Submitted works (Student Papers)

Integrity Flags

0 Integrity Flags for Review

No suspicious text manipulations found.

Our system's algorithms look deeply at a document for any inconsistencies that would set it apart from a normal submission. If we notice something strange, we flag it for you to review.

A Flag is not necessarily an indicator of a problem. However, we'd recommend you focus your attention there for further review.

Match Groups

- 139 Not Cited or Quoted 10%
  Matches with neither in-text citation nor quotation marks
- 0 Missing Quotations 0%
  Matches that are still very similar to source material
- 0 Missing Citation 0%
  Matches that have quotation marks, but no in-text citation
- 0 Cited and Quoted 0%
  Matches with in-text citation present, but no quotation marks

Top Sources

7% Internet sources
7% Publications
0% Submitted works (Student Papers)

Top Sources

The sources with the highest number of matches within the submission. Overlapping sources will not be displayed.

1	Internet	
ikee.lib.auth.gr		<1%
2	Internet	
www.slideshare.net		<1%
3	Internet	
erewhon.superkuh.com		<1%
4	Internet	
www.dtic.mil		<1%
5	Internet	
www.scribd.com		<1%
6	Publication	
Wolfgang Hauschild, Eberhard Lemke. "High-Voltage Test and Measuring Techniq...		<1%
7	Internet	
www.coursehero.com		<1%
8	Internet	
pdfcoffee.com		<1%
9	Internet	
es.scribd.com		<1%
10	Internet	
eprints.undip.ac.id		<1%

11	Publication	
Gaseous Dielectrics IX, 2001.		<1%
12	Publication	
Dimitrios Kokkinos. "Lightning protection system components standards in IEC 6...		<1%
13	Publication	
Shen, Shuhang. "Study of Prebreakdown and Breakdown Mechanisms of Transfor...		<1%
14	Publication	
Pavlos K. Samaras, Evangelos T. Staikos, Zacharias G. Datsios, Pantelis N. Mikropo...		<1%
15	Internet	
link.springer.com		<1%
16	Publication	
Yu, Haichuan. "Effects of Field Uniformity on Breakdown Characteristics of Transf...		<1%
17	Publication	
Vladimir V. Bolotin. "Mechanics of Fatigue", CRC Press, 2020		<1%
18	Internet	
ntnuopen.ntnu.no		<1%
19	Internet	
patents.justia.com		<1%
20	Internet	
steamradio.com		<1%
21	Publication	
Electrohydrodynamics, 1998.		<1%
22	Publication	
Vasily Y. Ushakov. "Insulation of High-Voltage Equipment", Springer Science and ...		<1%
23	Publication	
J. J. Shi. "Mitigating plasma constriction using dielectric barriers in radio-frequenc...		<1%
24	Publication	
E KUFFEL. "Generation of high voltages", High Voltage Engineering Fundamentals...		<1%

25	Internet	
essay.utwente.nl		<1%
26	Publication	
Congfu Ran, Xiongfeng Zhou, Kun Liu. "Insights into the mechanisms of plasma p...		<1%
27	Internet	
id.scribd.com		<1%
28	Publication	
L. Ashok Kumar, S. Albert Alexander. "Computational Paradigm Techniques for En...		<1%
29	Publication	
Dinan Wang. "Modeling of Electrokinetically Driven Flow Mixing Enhancement in ...		<1%
30	Publication	
Li-Yan Zhu. "ESD damage by directly arcing to a MR head", Electrical Overstress/El...		<1%
31	Internet	
www.bpasjournals.com		<1%
32	Publication	
Chachaia, Fernando Hausse. "Lightning Protection of Thatched Roofed Structures...		<1%
33	Publication	
M. Abdel-Salam, P. Weiss, B. Lieske. "Discharges in air from point electrodes in th...		<1%
34	Internet	
studyres.com		<1%
35	Publication	
Chenguo Yao, Zhongyong Zhao, Chengxiang Li, Xiaohan Chen, Yajun Zhao, Xiaozh...		<1%
36	Publication	
Dingchen Li, Chuan Li, Menghan Xiao, Li Jiawei, Zhiwen Yang, Qixiong Fu, Ming Zh...		<1%
37	Publication	
He, . "Design of Low-Voltage and Low-Distortion CMOS RF Integrated Circuits Usi...		<1%
38	Publication	
John Bird, John Bird. "Basic Engineering Mathematics", Routledge, 2019		<1%

39	Publication	Pantelis N. Mikropoulos, Petros P. Tsouris, Michalis K. Angeli, Fotini C. Knai. "Expe... <1%
40	Publication	Shilong Huang, Yunpeng Liu, Shaoshuai Chen, Guangyang Zhou, Wenbing Zhuan... <1%
41	Internet	demo.bharathuniv.ac.in <1%
42	Publication	J.L. Suthar, J.R. Laghari, T.J. Saluzzo. "Usefulness of SPICE in high voltage engineer... <1%
43	Internet	archive.org <1%
44	Internet	eurovolt.eu <1%
45	Internet	fr.slideshare.net <1%
46	Internet	pure-oai.bham.ac.uk <1%
47	Internet	www.rcet.org.in <1%
48	Internet	www.science.gov <1%
49	Publication	Min Hur. "Improvement of luminous efficacy in plasma display panels by a count... <1%
50	Publication	"Complex Dynamics of Traffic Management", Springer Science and Business Medi... <1%
51	Publication	I. Fofana, A. Beroual. "A model for long air gap discharge using an equivalent elec... <1%

ANNEX

Sample Experimental Data

Date	Levels	Pressure (mmHg)	Temperature (°C)	Absolute humidity h (gr/m³)	δ	κ	Polarity	t_{max}	R_f (Ω)	R_H (Ω)	R_t (Ω)	C_f (pF)	C_c (μF)	Stages	η (theor)	η (meas)
Sunday, December 1, 2024		760.50	16.00	10.33	1.01	0.99	Positve	2.15	34.20	1500.00	511.00	200.00	0.14	10.00	0.9593	0.9600

No.	U_0 (kV$_{dc}$)	Calculations							Measurements	1	2	3	4	5	6	7	8	9	10	11	12	13	14	15	16	17	18	19	20
1	61.50	P (%)	U_p (V)	t_l (μs)	U_l (V)	t_b (μs)	$U_{J/p}$ (V)	I_p (A)	t_b (μs)										12.79										
		5.00	379.05	#DIV/0!	-4.86	12.79	248.00	1240.00	U_p (V)	379.00	380.00	379.00	379.00	379.00	379.00	379.00	379.00	379.00	379.00	379.00	379.00	379.00	379.00	379.00	379.00	379.00	379.00	379.00
		$U_{p,th}$ (kV)	σ_{UP} (%)	σ_{tl} (%)	σ_{Ul} (%)	σ_{tb} (%)	$\sigma_{UJ/p}$ (%)	σ_{Ip} (%)	I_p (A)										1240.00										
		590.40	0.06	#DIV/0!	-447.21	#DIV/0!	#DIV/0!	#DIV/0!	$U_{J/p}$ (V)										248.00										
		591.29							t_l (μs)																				
		η	0.9614						U_l (V)	0.00	0.00	0.00	0.00	0.00	0.00	0.00	0.00	0.00	-97.16	0.00	0.00	0.00	0.00	0.00	0.00	0.00	0.00	0.00
2	62.00	P (%)	U_p (V)	t_l (μs)	U_l (V)	t_b (μs)	$U_{J/p}$ (V)	I_p (A)	t_b (μs)	3.95		3.60	9.30	6.24			6.92	4.45		11.15						6.13		
		40.00	380.75	#DIV/0!	-20.54	6.47	271.00	1353.75	U_p (V)	382.00	379.00	383.00	379.00	379.00	380.00	380.00	380.00	382.00	380.00	380.00	382.00	382.00	382.00	382.00	382.00	379.00	380.00	380.00
		$U_{p,th}$ (kV)	σ_{UP} (%)	σ_{tl} (%)	σ_{Ul} (%)	σ_{tb} (%)	$\sigma_{UJ/p}$ (%)	σ_{Ip} (%)	I_p (A)	1460.00		1460.00	1325.00	1315.00			1345.00	1390.00		1210.00						1325.00		
		595.20	0.35	#DIV/0!	-138.85	40.90	5.89	6.10	$U_{J/p}$ (V)	292.00		290.00	265.00	267.00			269.00	278.00		242.00						265.00		
		593.94							t_l (μs)																				
		η	0.9580						U_l (V)	-32.11	0.00	-29.36	-72.91	-49.94	0.00	0.00	-55.08	-36.03	0.00	-86.33	0.00	0.00	0.00	0.00	0.00	0.00	-49.06	0.00	0.00
3	62.50	P (%)	U_p (V)	t_l (μs)	U_l (V)	t_b (μs)	$U_{J/p}$ (V)	I_p (A)	t_b (μs)			6.50		4.06		10.82		3.56										
		20.00	383.70	#DIV/0!	-9.97	6.23	276.25	1381.25	U_p (V)	383.00	383.00	387.00	383.00	386.00	388.00	384.00	384.00	383.00	383.00	383.00	383.00	383.00	383.00	383.00	383.00	383.00	383.00	383.00
		$U_{p,th}$ (kV)	σ_{UP} (%)	σ_{tl} (%)	σ_{Ul} (%)	σ_{tb} (%)	$\sigma_{UJ/p}$ (%)	σ_{Ip} (%)	I_p (A)			1375.00		1450.00		1230.00		1470.00										
		600.00	0.39	#DIV/0!	-228.52	53.12	7.88	7.88	$U_{J/p}$ (V)			275.00		290.00		246.00		294.00										
		598.55							t_l (μs)																				
		η	0.9577						U_l (V)	0.00	0.00	-52.32	0.00	-33.27	0.00	-84.59	0.00	-29.26	0.00	0.00	0.00	0.00	0.00	0.00	0.00	0.00	0.00	0.00	0.00
4	63.00	P (%)	U_p (V)	t_l (μs)	U_l (V)	t_b (μs)	$U_{J/p}$ (V)	I_p (A)	t_b (μs)									7.60					8.83	5.11				
		15.00	387.95	#DIV/0!	-8.68	7.18	275.33	1376.67	U_p (V)	388.00	388.00	388.00	388.00	388.00	388.00	388.00	388.00	387.00	388.00	388.00	388.00	388.00	390.00	386.00	388.00	388.00	388.00	388.00
		$U_{p,th}$ (kV)	σ_{UP} (%)	σ_{tl} (%)	σ_{Ul} (%)	σ_{tb} (%)	$\sigma_{UJ/p}$ (%)	σ_{Ip} (%)	I_p (A)									1365.00					1365.00	1400.00				
		604.80	0.18	#DIV/0!	-250.28	26.41	1.47	1.47	$U_{J/p}$ (V)									273.00					273.00	280.00				
		605.17							t_l (μs)																				
		η	0.9606						U_l (V)	0.00	0.00	0.00	0.00	0.00	0.00	0.00	0.00	-61.26	0.00	0.00	0.00	0.00	-70.52	-41.84	0.00	0.00	0.00	0.00	0.00

Decay probability curve data

Decay Probability Curve						
No.	Up,th (kV)	P (%)	Hm/a	Rank	Condition	N/dist
0	547.20	0	549.60			0.06
0	552.00	0	554.40			0.10
0	556.80	0	559.20			0.19
0	561.60	0	564.00			0.33
0	566.40	0	568.80			0.55
0	571.20	0	573.60			0.90
0	576.00	0	578.40			1.44
0	580.80	0	583.20			2.24
0	585.60	0	588.00			3.38
1	590.40	5	592.80	5.00	588.00	4.96
2	595.20	40	597.60	10.00	592.80	7.08
3	600.00	20	602.40	15.00	592.80	9.83
4	604.80	15	609.60	20.00	609.60	13.29
5	614.40	20	619.20	25.00	619.20	22.51
6	624.00	25	628.80	30.00	628.80	34.54
7	633.60	65	638.40	35.00	628.80	48.40
8	643.20	80	648.00	40.00	628.80	62.45
9	652.80	65	657.60	45.00	628.80	75.01
10	662.40	70	667.20	50.00	628.80	84.90
	672.00	90.00	681.60	55.00	628.80	91.77
	691.20	90.00	700.80	60.00	628.80	98.23
	710.40	100.00	720.00	65.00	628.80	99.76
	729.60	100.00	364.80	70.00	657.60	99.98
				75.00	667.20	
				80.00	667.20	
				85.00	667.20	
				90.00	667.20	
				95.00	667.20	
				100.00	667.20	
				Average If	634.68	
				σ_{if} (%)	4.23	

U_{th} (kV)	U_{50} (Kv)	U_{st} (Kv)
582.04	634.68	687.32
559.96	4.23	

Summary of results

Summary of Results															
No	Uo (kV)	P (%)	Up,th (kV)	Uinst,w (kV)	σUi(%)	t_l (µs)	σ_{tl} (%)	$U_{l,w}$ (kV)	σ_{Ul} (%)	tb (µs)	σtb(%)	$U_{lp,w}$ (kV)	$\sigma_{U,lp}$ (%)	I_p (kA)	σ_{Ip} (%)
1	61.50	5	590.40	591.29	0.06	#DIV/0!	#DIV/0!	-7.58	-447.21	12.79	#DIV/0!	386.86	#DIV/0!	1.24	#DIV/0!
2	62.00	40	595.20	593.94	0.35	#DIV/0!	#DIV/0!	-32.04	-138.85	6.47	40.90	422.74	5.89	1.35	6.10
3	62.50	20	600.00	598.55	0.39	#DIV/0!	#DIV/0!	-15.56	-228.52	6.23	53.12	430.93	7.88	1.38	7.88
4	63.00	15	604.80	605.17	0.18	#DIV/0!	#DIV/0!	-13.54	-250.28	7.18	26.41	429.50	1.47	1.38	1.47
5	64.00	20	614.40	615.70	0.25	#DIV/0!	#DIV/0!	-14.99	-212.11	5.81	28.32	437.17	3.38	1.40	3.38
6	65.00	25	624.00	622.18	0.15	#DIV/0!	#DIV/0!	-22.03	-190.06	6.80	38.98	447.39	4.58	1.43	4.58
7	66.00	65	633.60	633.72	0.37	#DIV/0!	#DIV/0!	-49.61	-88.72	5.76	40.44	463.66	4.47	1.49	4.48
8	67.00	80	643.20	643.16	0.14	#DIV/0!	#DIV/0!	-56.84	-59.01	5.24	27.51	483.58	5.35	1.45	5.35
9	68.00	65	652.80	652.67	0.31	#DIV/0!	#DIV/0!	-45.06	-84.70	5.04	33.01	509.62	5.96	1.48	5.96
10	69.00	70	662.40	660.32	0.11	#DIV/0!	#DIV/0!	-62.43	-83.85	6.48	45.79	492.49	9.40	1.51	9.40
11	70.00	90	672.00	669.91	0.23	#DIV/0!	#DIV/0!	-53.20	-48.85	4.15	34.28	526.13	9.26	1.54	9.29
12	72.00	90	691.20	689.49	0.33	#DIV/0!	#DIV/0!	-47.61	-39.77	3.59	19.78	579.34	4.15	1.60	4.15
13	74.00	100	710.40	705.95	0.25	#DIV/0!	#DIV/0!	-50.76	-25.28	3.35	25.95	565.63	6.74	1.66	7.02
14	76.00	100	729.60	725.68	0.32	#DIV/0!	#DIV/0!	-23.07	-107.46	2.95	23.80	551.90	4.43	1.72	4.27
15	78.00	100	748.80	738.94	2.76	#DIV/0!	#DIV/0!	-23.59	-110.08	2.94	29.61	560.48	4.02	1.79	3.97
16	80.00	100	768.00	759.69	0.73	#DIV/0!	#DIV/0!	-19.44	-110.62	2.35	30.68	546.29	1.54	1.85	1.54
17	83.00	100	796.80	772.79	0.78	#DIV/0!	#DIV/0!	-7.50	-178.20	1.74	7.30	542.86	3.45	1.94	3.41
18	86.00	100	825.60	797.12	0.62	#DIV/0!	#DIV/0!	-7.97	-178.36	1.79	8.44	556.90	3.88	2.03	3.88
19	90.00	100	864.00	821.46	1.69	#DIV/0!	#DIV/0!	-7.68	-180.08	1.64	16.08	568.75	3.92	2.15	3.92
20															

Curve characteristics table

Curve Characterisitcs Table															
No	Uo (kV)	P (%)	$U_{p,th}$ (kV)	$U_{inst,w}$ (kV)	σ_{Ui}(%)	t_b (µs)	σ_{tb}(%)	U-T	1/tb	U-T/U0	U/Uth	v (m/µs)	U-T/U50	Uinst/U50	Uinst/U0
1	61.50	5	590.40	591.29	0.06	12.79	#DIV/0!	590.40	0.08	1.05	1.05	0.00	0.93	0.93	1.06
2	62.00	40	595.20	593.94	0.35	6.47	40.90	595.20	0.15	1.06	1.06	0.00	0.94	0.94	1.06
3	62.50	20	600.00	598.55	0.39	6.23	53.12	600.00	0.16	1.07	1.07	0.00	0.95	0.94	1.07
4	63.00	15	604.80	605.17	0.18	7.18	26.41	604.80	0.14	1.08	1.08	0.00	0.95	0.95	1.08
5	64.00	20	614.40	615.70	0.25	5.81	28.32	614.40	0.17	1.10	1.10	0.00	0.97	0.97	1.10
6	65.00	25	624.00	622.18	0.15	6.80	38.98	624.00	0.15	1.11	1.11	0.00	0.98	0.98	1.11
7	66.00	65	633.60	633.72	0.37	5.76	40.44	633.60	0.17	1.13	1.13	0.00	1.00	1.00	1.13
8	67.00	80	643.20	643.16	0.14	5.24	27.51	643.20	0.19	1.15	1.15	0.00	1.01	1.01	1.15
9	68.00	65	652.80	652.67	0.31	5.04	33.01	652.80	0.20	1.17	1.17	0.00	1.03	1.03	1.17
10	69.00	70	662.40	660.32	0.11	6.48	45.79	662.40	0.15	1.18	1.18	0.00	1.04	1.04	1.18
11	70.00	90	672.00	669.91	0.23	4.15	34.28	672.00	0.24	1.20	1.20	0.00	1.06	1.06	1.20
12	72.00	90	691.20	689.49	0.33	3.59	19.78	691.20	0.28	1.23	1.23	0.00	1.09	1.09	1.23
13	74.00	100	710.40	705.95	0.25	3.35	25.95	710.40	0.30	1.27	1.27	0.00	1.12	1.11	1.26
14	76.00	100	729.60	725.68	0.32	2.95	23.80	729.60	0.34	1.30	1.30	0.00	1.15	1.14	1.30
15	78.00	100	748.80	738.94	2.76	2.94	29.61	748.80	0.34	1.34	1.34	0.00	1.18	1.16	1.32
16	80.00	100	768.00	759.69	0.73	2.35	30.68	768.00	0.42	1.37	1.37	0.00	1.21	1.20	1.36
17	83.00	100	796.80	772.79	0.78	1.74	7.30	772.79	0.57	1.38	1.38	0.00	1.22	1.22	1.38
18	86.00	100	825.60	797.12	0.62	1.79	8.44	797.12	0.56	1.42	1.42	0.00	1.26	1.26	1.42
19	90.00	100	864.00	821.46	1.69	1.64	16.08	821.46	0.61	1.47	1.47	0.00	1.29	1.29	1.47

Additional Data

Additional Data									
No	Uo (kV)	Uinst,w (kV)	$U_{,Ip,w}$ (kV)	I_p (kA)	Up/Ip (Ω)	U,Ip/Ip (Ω)	Up/U,Ip	Ip/Up (mS)	Ip/U,Ip (mS)
1	61.50	591.29	386.86	1.24	476.85	311.99	1.53	2.10	3.21
2	62.00	593.94	422.74	1.35	438.74	312.27	1.40	2.28	3.20
3	62.50	598.55	430.93	1.38	433.34	311.99	1.39	2.31	3.21
4	63.00	605.17	429.50	1.38	439.59	311.99	1.41	2.27	3.21
5	64.00	615.70	437.17	1.40	439.40	311.99	1.41	2.28	3.21
6	65.00	622.18	447.39	1.43	433.88	311.99	1.39	2.30	3.21
7	66.00	633.72	463.66	1.49	426.31	311.91	1.37	2.35	3.21
8	67.00	643.16	483.58	1.45	444.13	333.93	1.33	2.25	2.99
9	68.00	652.67	509.62	1.48	441.34	344.60	1.28	2.27	2.90
10	69.00	660.32	492.49	1.51	437.42	326.24	1.34	2.29	3.07
11	70.00	669.91	526.13	1.54	434.92	341.58	1.27	2.30	2.93
12	72.00	689.49	579.34	1.60	430.46	361.69	1.19	2.32	2.76
13	74.00	705.95	565.63	1.66	424.46	340.09	1.25	2.36	2.94
14	76.00	725.68	551.90	1.72	420.78	320.01	1.31	2.38	3.12
15	78.00	738.94	560.48	1.79	413.73	313.81	1.32	2.42	3.19
16	80.00	759.69	546.29	1.85	411.20	295.69	1.39	2.43	3.38
17	83.00	772.79	542.86	1.94	398.41	279.87	1.42	2.51	3.57
18	86.00	797.12	556.90	2.03	392.32	274.09	1.43	2.55	3.65
19	90.00	821.46	568.75	2.15	381.24	263.96	1.44	2.62	3.79

Average U_p/I_p	1.36
$\sigma_{Up/Ip}$ (%)	5.85
Average $U_{,Ip}/I_p$	2.35
$\sigma_{U,Ip/Ip}$ (%)	5.12
Average $U_p/U_{,Ip}$	3.20
σUp/U,Ip (%)	8.10